

Scenario Predict-then-Optimize for Data-Driven Online Inventory Routing

Menglei Jia

Department of Management Science, Antai College of Economics and Management, Shanghai Jiao Tong University, China

Albert H. Schrottenboer

Operations, Planning, Accounting, and Control Group, School of Engineering, Eindhoven University of Technology, the Netherlands

Feng Chen

Sino-US Global Logistics Institute, Antai College of Economics and Management, Shanghai Jiao Tong University, China {fchen@sjtu.edu.cn}

Problem definition: The real-time joint optimization of inventory replenishment and vehicle routing is essential for cost-efficiently operating one-warehouse, multiple-retailer systems. This is complex, as future demand predictions should capture (auto)correlation and lumpy retailer demand, and based upon such predictions, inventory replenishment and vehicle routing decisions must be taken. Traditionally, such decisions are made by either making distributional assumptions or using machine-learning-based point forecasts. The former approach ignores nonstationary demand patterns, while the latter approach only provides a point forecast ignoring the inherent forecast error. Consequently, in practice, service levels often do not meet their targets, and truck fill rates fall short, harming the efficiency and sustainability of daily operations. **Methodology/results:** We propose Scenario Predict-then-Optimize. This fully data-driven approach for online inventory routing consists of two subsequent steps at each real-time decision epoch. The *scenario-predict* step exploits neural networks – specifically multi-horizon quantile recurrent neural networks – to predict future demand quantiles, upon which we design a scenario sampling approach. The subsequent *scenario-optimize* step then solves a scenario-based two-stage stochastic programming approximation. Results show that our approach outperforms a classic prediction-focused learning approach, distributional approaches, empirical sampling methods, residuals-based sample average approximation, and a state-of-the-art decision-focused learning approach. We show this both on synthetic data and large-scale real-life data from our industry partner. **Implications:** Our approach is appealing to practitioners. It is fast, does not rely on any distributional assumption, and does not face the burden of single-scenario forecasts. It also outperforms residuals-based scenario generation techniques. We show it is robust for various demand and cost parameters, enhancing the efficiency and sustainability of daily inventory replenishment and truck routing decisions. Finally, scenario Predict-then-Optimize is general and can be easily extended to account for other operational constraints, making it a useful tool in practice.

Key words: inventory routing; data-driven optimization; prediction-focused learning; machine learning; stochastic optimization

1. Introduction

Optimal inventory replenishment and truck routing in one-warehouse, multiple-retailer systems is fundamental for supply chain management (Bertazzi 2008). In 2021, total operating expenses and end-of-year inventories of U.S. retailer businesses were \$1,417,106 billion and \$655.923 billion, respectively, accounting

for 21.73% and 10.06% of total sales (U.S. Census Bureau 2022). Traditionally, inventory replenishment and truck routing are controlled separately. Replenishment follows a relatively static ordering logic including base-stock and order-up-to policies (Huh and Janakiraman 2008, Xu et al. 2011). Only after the replenishment quantities have been determined, transportation costs associated with the distribution via truck routes are minimized. Although simple and widely used in practice, this process exhibits two apparent drawbacks: The disintegration of inventory replenishment and truck routing leading to suboptimal joint decisions, and secondly, the inability to act dynamically upon demand shifts, trends, and disruptions due to the static ordering logic. However, this traditional perspective is subject to change. Widespread data availability and efficient IT systems increasingly motivate retailers to adopt a dynamic decision-making process that *integrates* replenishment and truck routing decisions based upon the latest demand information.

Real-time inventory replenishment and truck routing are studied in (variants of) the Stochastic Inventory Routing Problem (Coelho et al. 2014b). Generally speaking, these problems consider a depot, at which capacitated trucks are stationed, and a set of geographically scattered retailers each facing stochastic demand. Using truck routes to replenish the retailers' inventory, the goal is to minimize the expected sum of inventory and transportation costs while meeting a service-level criterion at each retailer. To do so efficiently, decision-makers rely on the quality of the predictions of future retailer demand. Indeed, such demand predictions must subsequently be merged with optimization tools to transfer the prediction into actual real-time inventory replenishment and truck routing decisions.

However, integrating prediction and optimization is complex. Existing research has focused on imposing distributional (robust) assumptions on retailer demand (see, e.g., Adelman 2004, Kleywegt et al. 2004, Cui et al. 2023). However, demand is nonstationary and (auto)correlated in practice, which invalidates making distributional assumptions. Alternatively, researchers develop machine-learning-based point forecasts of future retailer demand (see, e.g., the prediction approach in Huber and Stuckenschmidt 2020). While circumventing the drawbacks of (static) distributional assumptions, solely basing a decision on a single point forecast leads to overly specific decisions by ignoring forecast errors.

As a solution, we introduce "Scenario Predict-then-Optimize" (ScenPO), a novel data-driven prediction and optimization approach for integrated, data-driven inventory replenishment and truck-routing decisions. Our ScenPO approach neither relies on making distributional assumptions nor on a single point forecast. It consists of a distribution-free *scenario-predict* step, which generates data-driven future demand scenarios for individual retailers, and a *scenario-optimize* step that leverages powerful stochastic programming approaches. For the prediction step, we propose using a Multi-Horizon Quantile Recurrent Neural Network (MQRNN), which predicts future demand quantiles for a given number of periods based on past retailer demand observations (Wen et al. 2017). We use these predicted quantiles to sample the scenarios needed for the scenario-optimize step. The scenario-optimize step then solves a multiperiod stochastic

inventory routing problem based on the data-driven scenarios from the scenario-predict step. It determines joint inventory-replenishment and truck-routing decisions for a given number of future periods, of which we only execute the decisions until the next decision epoch. In this way, we do not suffer from the inherent risk of working with single-scenario forecasts. Using stochastic programming, we automatically find a solution with the lowest expected cost that hedges the forecast error. Moreover, we can leverage a suite of efficient solution approaches for such models, including scenario-decomposition methods such as progressive hedging. It is worth noting that ScenPO is generic and applies to any setting that combines demand forecasting and combinatorial optimization.

Our ScenPO approach is an alternative to so-called decision-focused learning approaches – that integrates learning and optimization and is also called end-to-end learning – for solving complex online combinatorial optimization problems. Instead of solely focusing on minimizing a prediction error, decision-focused learning approaches aim to minimize the expected cost of the resulting decisions (see, e.g., Elmachtoub and Grigas 2022, Mandi et al. 2023). For several reasons, such methods cannot be applied to our setting efficiently. A first stream of methods focus on the implementation of differentiable optimization layers, relying on a useful approximation of the optimization problem differential in the backward pass. Almost all existing works consider the setting where uncertainty solely lies in the objective function; however, many cases, including ours, have uncertainty in their constraints which invalidates such approaches (Kotary et al. 2021). While it is also possible to consider uncertainty in the constraints (see, e.g., Paulus et al. 2021), the learning problem has not yet been well-defined. As a consequence, it is not so effective for complex combinatorial optimization problems with dense solutions and many constraints and variables including the data-driven online inventory routing problem that we study in this paper (Coelho et al. 2014b). A second stream develops so-called surrogate loss functions with appealing computational properties (see, e.g., Sahay and Ierapetritou 2016, Ye and You 2016) – which are effective in many contexts but ignore the vast stream of literature and knowledge on real-time integrated inventory replenishment and truck routing decisions.

As an efficient alternative to decision-focused learning, our ScenPO method does not learn the optimization performance but relies on stochastic programming to automatically hedge against forecast errors while considering data-driven future demand scenarios. In ScenPO, the prediction step can be performed independently of the optimization step, which is computationally appealing. We exploit stochastic programming to obtain a solution that minimizes the expected costs among the predicted scenarios. In our approach, the prediction step does not require evaluating optimization methods. Moreover, as our approach is derivative-free on the optimization problem, we also eradicate the need to develop surrogate models with favorable properties. Our ScenPO approach can thus be classified as a prediction-focused learning approach, though we reserve this term in our paper for approaches considering point forecasts

to enhance readability. To the best of the authors' knowledge, our ScenPO is the first approach that integrates demand prediction and optimization in the context of joint replenishment and truck routing in data-driven online inventory routing.

In ScenPO, the prediction-step does not follow the recent trend of developing scenarios in a residuals-based manner. For example, Kannan et al. (2022) first train a prediction model to obtain a point prediction, and then the residuals obtained during training are scaled and added to that prediction to construct scenarios. The predictors (residuals) can be of different designs to improve performance. Our ScenPO approach, and specifically the MQRNN we use, is an alternative approach, as it is based on forecasting demand quantiles which provide a robust characterization of the distribution of stochastic variables. This in turn allows us to generate demand forecasts scenarios in a robust way.

We propose several variations of ScenPO to test and assess its different components structurally. First, besides considering MQRNNs, we also consider Long Short-Term Memory Neural Networks (LSTM) in our scenario-predict step and provide an associated scenario-sampling strategy. For the scenario-optimize step, we consider two distinct stochastic programming formulations. First, a single-stage (*SS*) formulation assumes that the replenishment and truck-routing decisions are made in the first stage, while the second stage only evaluates the proposed solutions over the scenarios. Second, a two-stage (*TS*) formulation allows for different replenishment and truck-routing decisions in all future periods. Both formulations employ a tailored matheuristic inspired by Solyalı and Süral (2022) to solve the stochastic optimization problems. For the second formulation, we also employ progressive hedging (Rockafellar and Wets 1991) to enhance its computational tractability further.

We evaluate our ScenPO approach (and its variations) compared to various benchmarks, both on the optimization and on the prediction side. That is, we consider various scenario sampling techniques that afterward use our scenario-optimize step. These are (i) a maximum likelihood approach that fits the best distribution, (ii) empirical sampling approaches, (iii) various standard prediction-focused learning approaches utilizing point forecasts, (iv) various state-of-the-art residuals-based data-driven sample average approximation approaches proposed by Kannan et al. (2022), (v) a traditional Holt-Winters exponential smoothing approach, and (vi) a standard quantile regression model. In addition, we compare ScenPO to a state-of-the-art decision-focused learning approach called CombOptNet, as proposed by Paulus et al. (2021). First, we assess all the methods on synthetic data to control the degree of demand nonstationarity. Afterward, we utilize large-scale real-life data regarding the aftersales of spare parts from our industry partner, SAIC Volkswagen Automotive Co., Ltd., in China in 2020.

Our results show that ScenPO using MQRNN combined with the *SS* stochastic programming formulation performs robustly over all our instances and significantly outperforms all other methods. Our best ScenPO approach reduces the gap between an oracle solver with perfect demand knowledge and

the expected value solution by 61.60% on average, whereas the best “classic” prediction-focused learning paradigm only reduces this gap by 30.20% on average. Notably, the state-of-the-art sample average approximation approach by Kannan et al. (2022) reduces this gap by 51.00%, whereas the standard quantile regression reduces this gap by 55.60% on average. More specifically, we observe that the residuals-based approach can match the performance of our ScenPO for simple data patterns that are relatively easy to predict. However, when the data patterns become more complex, especially as observed in our real-life data, the residuals-based approach cannot match our ScenPO (and other quantile-based approaches). This confirms that quantile regression is a robust basis for scenario generation within our ScenPO framework in the context of online data-driven inventory routing.

The main contributions are summarized as follows:

- We introduce Scenario Predict-then-Optimize for joint distribution and replenishment in one-warehouse-multiple-retailer systems, also known as data-driven online inventory routing. It combines prediction and optimization, provides better operational decisions, and can be easily implemented in practice. It consists of a *scenario-predict* step, which provides distribution-free data-driven scenarios, which are then exploited by the *scenario-optimize* step. Here, stochastic programming is employed to make joint replenishment and distribution decisions.
- In the context of data-driven online inventory routing, this is the first fully integrated prediction and optimization approach that does not make distributional assumptions on the input data nor works with single-point forecasts.
- We detail how to employ Multi-Horizon Quantile Recurrent Neural Networks as part of our scenario-predict step, and we provide two distinct two-stage stochastic programming formulations for the scenario-optimize step. For the latter part, we provide tailored heuristic algorithms and utilize progressive hedging to further enhance the computational performance of ScenPO.
- Both on synthetic data and large-scale real-life data from SAIC Volkswagen Automotive Co., Ltd., we show that ScenPO outperforms a range of benchmark approaches, including single-scenario prediction-focused learning, empirical sampling techniques, state-of-the-art residuals-based data-driven sample average approximation, and a state-of-the-art decision-focused learning approach using CombOptNet.
- We evaluate the strengths and weaknesses of different state-of-the-art approaches through extensive numerical experiments, providing a better understanding of which paradigms are suitable for particular use cases. Our extensive numerical experiments demonstrate the value of using quantile-based scenario generation approaches over residuals-based scenario-generation approaches within ScenPO. To the best of our knowledge, this has not yet been studied in the inventory routing literature and is important to consider in the development of online data-driven algorithms.

The remainder of the paper is organized as follows. In Section 2, we review the related literature. The problem description and associated Markov decision process formulation can be found in Section 3. Subsequently, Section 4 details our ScenPO approach, and Section 5 provides several algorithms for enhancing the efficiency of the scenario-optimize step. Computational experiments on synthetic and large-scale real-life data are provided in Section 6. We conclude our work and discuss future research avenues in Section 7.

2. Literature Review

The real-time joint distribution and replenishment of inventory in one-warehouse-multiple-retailer systems is often referred to as the Stochastic and Dynamic Inventory Routing Problem. In this work, we consider a new variant of this problem, which we call the Data-driven Online Inventory Routing Problem, which does not consider any distributional assumptions on retailer demands. Furthermore, we use the phrases “warehouse” and “retailer” in our paper, but this can also be interpreted as “depot” and “customer”, which are more commonly used in the vehicle routing literature.

The classic, deterministic inventory routing problem (IRP) integrates vehicle routing and inventory management. It is motivated by vendor-managed inventory settings and has a wide range of real-life applications, from retailer replenishment to aftersales logistics of spare parts (Andersson et al. 2010). The Stochastic Inventory Routing Problem (SIRP) refers to the problem with stochastic demand (see, e.g., Sonntag et al. 2023, Hasturk et al. 2024), and the Stochastic and Dynamic Inventory Routing Problem (SDIRP) refers to the problem in which information is revealed dynamically and decisions are made online. In our review, we focus solely on the SDIRP. For a more general, routing-oriented review, we refer the reader to the excellent review by Coelho et al. (2014b).

The SDIRP has been studied extensively. However, most studies make distributional assumptions for retailer demand. Jaillet et al. (2002) concern the SDIRP in which a commodity has to be distributed to retailers repeatedly over a long time horizon, which they solve using incremental cost approximations. Kleywegt et al. (2002) formulate the inventory routing problem with direct deliveries as a Markov decision process and use dynamic programming techniques to approximate a decomposed value function. That has been extended by Kleywegt et al. (2004), in which multiple retailers are considered in a single-vehicle route. Adelman (2004) also formulate the SDIRP as a Markov decision process and solve it by approximating the future costs of current actions using optimal dual prices of a linear program. Coelho et al. (2014a) are the first considering SDIRP without distributional assumptions, where two different policies, proactive and reactive, are proposed to deal with dynamic demand. In the proactive policy, they make decisions based on an oracle forecast, solving a deterministic equivalent formulation. Under the reactive policy, they generate decisions based on the (s, S) policy, where s is calculated according to the demand distribution and can be updated at the beginning of each period to deal with dynamic demand. Achamrah et al. (2022) adopt a similar approach to the reactive policy where they consider transshipment and substitution to

mitigate shortages. Crama et al. (2018) similarly consider different demand distributions over time and develop different solution methods for SDIRP for perishable products. Except for the proactive policy of Coelho et al. (2014a), all other works, despite considering dynamic demand, still rely on distributional assumptions and solve the dynamic problem by considering a newly fitted distribution on a rolling basis. The most recent work is by Cui et al. (2023), which employs a distributional robust optimization approach with a moment-based ambiguity set. However, although they no longer specify the distribution, corresponding moment information still needs specification. Moreover, by exploring (distributionally) robust optimization, they minimize the expected cost for the worst-case distribution within the ambiguity set and not, as in our ScenPO, minimize the expected cost.

Slightly different works are Hvattum and Løkketangen (2009) and Hvattum et al. (2009). They approximate the infinite horizon Markov decision process by solving a finite scenario tree problem on a rolling basis. However, scenario tree generation still requires a distributional assumption — they are generated by random sampling from a distribution. Different distribution assumptions for different periods can formulate dynamic demand. However, determining the underlying distributions for each future period is a fundamental yet tricky issue. The mentioned works either specify the same distribution for each period or randomly generate distribution parameters, neglecting the sequential relationship among the demand in different periods as observed in practice. The work of Greif et al. (2024) is notable, but differs from our work on a few important aspects. They solve the SDIRP through an end-to-end learning idea by adopting the ideas of Parmentier (2021), Dalle et al. (2022), Parmentier (2022), and Baty et al. (2024), in which dynamic routing problems are transferred into single-period price-collecting routing problem, where the “prices” are learned by a machine learning predictor. However, Greif et al. (2024) consider a single vehicle only, and more importantly, only consider replenishing retailers towards their full capacity. In that way, the inventory replenishment quantity is not actively decided upon, which significantly reduces decision complexity. Our approach allows for replenishing any amount of inventory. Indeed, our ScenPO approach leverages a data-driven approach that first captures future information based on historical demand through a *scenario-predict* step without any distributional assumption and then gives an approximate solution through a *scenario-optimize* step to hedge against the prediction error by minimizing the expected finite horizon cost using stochastic programming. It can be applied to any setting that combines forecasting and combinatorial optimization and is a generic and relatively easy to apply.

Effective solution approaches for real-life stochastic problems involve prediction and optimization components. However, most studies treat prediction and optimization independently. For example, Keskin et al. (2023) adopt the classic prediction-focused learning framework to solve the waste collection problem with “touting” as a demand management technique, where retailers who have not yet placed an order can be actively encouraged to order a service sooner. The candidate touting retailers, i.e., the retailers likely to order soon, are determined based on the predicted fill rates by a forecasting model. Then, a multi-period

vehicle routing problem with touting is solved based on the predicted results. In recent years, an emerging topic has been decision-focused learning of prediction models based on optimization models. This stream of research focuses on training machine learning models to optimize the quality of the resulting decisions and, therefore, do not necessarily lead to the best point forecasts from a prediction perspective. Nevertheless, such studies are mostly limited to linear programming problems with uncertain parameters in the objective function, such as Wilder et al. (2019), Mandi and Guns (2020), and Elmachtoub and Grigas (2022). Liu and Grigas (2022) extend the work of Elmachtoub and Grigas (2022) to consider online contextual decision-making with resource constraints. However, even though their problem contains uncertainty in the constraints, the solution method is still based on the fundamental technique of Elmachtoub and Grigas (2022), transferring the constrained problem into a penalized version of the objective by introducing dual variables and using primal-dual methods. This approach applies to problems with specific structures and is not generalizable. Vlastelica et al. (2019), Ferber et al. (2020), and Mandi et al. (2020) have extended research into combinatorial optimization, but the optimization problems targeted are still limited to problems with uncertain parameters in the objective function. Although the current state-of-the-art can also differentiate mixed integer linear programming concerning constraints (Paulus et al. 2021), the architecture needs solutions to the problem for the training process, leading to solving many optimization problems in advance. This imposes a major computational burden on the efficiency of the method. Moreover, the state-of-the-art learning problem has not yet been well-defined in this setting, and thus, is not as effective for complex combinatorial optimization problems with dense solutions and many constraints and variables. We refer the interested reader to Kotary et al. (2021), Qi and Shen (2022), Mandi et al. (2023), Sadana et al. (2024) for more research in this area.

As far as we know, we are the first to generate scenarios for a stochastic optimization problem using quantiles predicted from MQRNN. The studies of Kim et al. (2023) and Doan et al. (2024) are most relative, with quantile-based scenario generation followed by stochastic optimization. However, the forecasting method is different. Kim et al. (2023) predicts quantiles using a quantile LSTM (QLSTM) (Wang et al. 2019), and Doan et al. (2024) use a TransLSTM (Song et al. 2022). Both networks generate multistep forecasts with a recursive strategy, that is, they train a model to predict the one-step-ahead estimate, and then iteratively feed this estimate back as the ground truth to forecast longer horizons. In the field of forecasting, Chevillon (2007) showed that the direct strategy, where a model directly predicts multistep forecasts, as we use within ScenPO with the MQRNN, is less biased, more stable, and more robust to model misspecification. In addition, the context of their study is also completely different, that is, they study an energy management problem that only considers day-ahead scheduling based on the forecasted energy demands and generations, which is a single-stage stochastic problem. However, the data-driven online IRP requires making decisions for multiple look-ahead periods, which is a multi-stage optimization problem and more complex to analyze.

The scenario-predict step of ScenPO is related to research on time-series forecasting. Traditional time-series forecasting methods such as exponential smoothing or the use of autoregressive models such as ARMA and its variants are widespread. In the last decade, deep learning-based forecasting has shown great promise compared to the more traditional approaches. For example, Cai et al. (2019) compare two classical deep neural network models with the seasonal ARIMAX model in day-ahead multi-step load forecasting in commercial buildings, and the best-performing deep learning model improves the forecasting accuracy by 22.6% compared to that of the seasonal ARIMAX. In the following, we introduce the main elements of deep learning relevant for ScenPO, and refer the reader to Chatfield (2000), De Gooijer and Hyndman (2006), and Lim and Zohren (2021) for more information on time-series forecasting.

Recurrent Neural Network (RNN) is a recursive neural network that takes sequences as input. It has advantages in learning the nonlinear characteristics of sequences and is widely applied in various time-series forecasting. The Long-Short Term Memory Network (LSTM) (Hochreiter and Schmidhuber 1997) and Gate Recurrent Unit Network (GRU) (Cho et al. 2014) are two popular variants of RNN. They addressed the issue of RNN that can only look back in time for limited timesteps due to the fed-back signal either vanishing or exploding (Staudemeyer and Morris 2019). Both LSTM and GRU provide point forecasts, however, and by the nature of being a prediction, they are surrounded by a prediction error. In addition, most deep learning forecasting can only predict a one-step-ahead estimate and then iteratively feed this estimate back as the ground truth to forecast longer time horizons (Wen et al. 2017). Such a process leads to prediction error accumulation - and is clearly not reliable enough to base decisions on. Wen et al. (2017) exploit the expressiveness and temporal nature of Sequence-to-Sequence Neural Network (Seq2Seq), the nonparametric nature of Quantile Regression (Koenker and Bassett Jr 1978), which estimates the conditional quantiles of the distribution of the response variable, i.e., the τ th conditional quantile of the distribution of Y given X , y^τ , satisfies $\mathbb{P}(Y \leq y^\tau | X) = \tau$, and the efficiency of Direct Multi-Horizon Forecasting, which directly predicts the multi-horizon estimates for each period instead of recursively predicting the one-step-ahead estimate. They propose a Multi-Horizon Quantile RNN (MQRNN) forecaster: a Seq2Seq framework that generates multi-horizon quantile forecasts, which does not make distributional assumptions, produces accurate probabilistic forecasts with sharp prediction intervals, and can directly predict multi-horizon with less bias, more stability, and more robustness. Therefore, we use MQRNN in our ScenPO approach to make probabilistic forecasts based on a large amount of historical data to obtain more robust results in the optimization phase. In our computational campaign, we also compare the usefulness of LSTM in the scenario-predict step of our ScenPO approach.

After the scenario-predict step, our ScenPO approach moves to the scenario-optimize step. For this, we employ two-stage stochastic programming. The Progressive Hedging Algorithm (PHA) is a horizontal decomposition method for large-scale problems proposed by Rockafellar and Wets (1991), which has theoretical convergence properties when all decision variables are continuous. It can be effectively used

as a heuristic when applied to problems with discrete decision variables, as in this study's case of data-driven online inventory routing. Whereas the PHA has applications in many supply chain management problems (Hvattum and Løkketangen 2009, Dong et al. 2015, Kim et al. 2015, Hu et al. 2019, Jalilvand et al. 2021, Dong et al. 2022), Hvattum and Løkketangen (2009) is the only work that has explored the PHA in the context of the stochastic inventory routing. We employ the PHA for the *TS* stochastic programming formulation within the scenario-optimize step of ScenPO.

3. Problem Description

This section introduces the data-driven online inventory routing problem as a Markov decision process. We first introduce the main system components. We consider an infinite discrete time horizon \mathcal{K} , where each $k \in \mathcal{K}$ is called a period. We consider retailers $\mathcal{N} = \{1, 2, \dots, N\}$ who each face stochastic demand, and a single warehouse $\{0\}$ with unlimited stock. We denote the retailers and the warehouse by the set \mathcal{N}^+ . In each period $k \in \mathcal{K}$, we denote the inventory at each retailer by $\mathcal{I}_k = \{I_k^1, \dots, I_k^N\}$, where $I_k^i \in \{-\infty, \dots, I^{\max}\}$. Here, I^{\max} is the inventory capacity at each retailer, and negative inventory implies backorders. Each retailer incurs per-unit holding costs h for inventory that carries over between periods, and per-unit backorder costs e for backlogged demand per period. To replenish inventory from the warehouse to the retailers, we use a homogeneous set of vehicles $\mathcal{V} = \{1, \dots, V\}$, where each vehicle $v \in \mathcal{V}$ has maximum capacity Q . Vehicles make, at most, a single replenishment route per period. Each replenishment route incurs variable transportation costs depending on the geographical location of the retailers.

The sequence of events in each period k is as follows. First, we observe inventory levels at the retailers, then we make a vehicle routing and replenishment decision that happens instantaneously, and afterward, the demand of period k occurs at each retailer.

The goal is to find a policy that, given past demand observations and current inventory levels at the retailers, determines how much inventory to replenish to each retailer with the available fleet of vehicles that minimizes the sum of expected holding, backorder, and transportation costs per period. In the following, we formally present the formulation of the Markov decision process.

In any period k , we let $\tilde{\mathcal{Y}}_{:k} = \{\tilde{Y}_{:k}^1, \dots, \tilde{Y}_{:k}^N\}$ denote the last L demand observations at the retailers. Here, $\tilde{Y}_{:k}^i = \{\tilde{y}_{k-1}^i, \tilde{y}_{k-2}^i, \dots, \tilde{y}_{k-L}^i\}$, where \tilde{y}_k^i denotes the realization of the random demand y_k^i at retailer i in period k . We assume the random variable y_k^i has nonnegative discrete support $\mathcal{Y} := \{0, 1, \dots, O\}$. The system state S_k is then denoted as $S_k = (\mathcal{I}_k, \tilde{\mathcal{Y}}_{:k})$, $S_k \in \mathcal{S} := \{\times_{i \in \mathcal{N}} \{-\infty, \dots, I^{\max}\}\} \times \{\times_{i \in \mathcal{N}} \times_{t \in \{k-1, k-2, \dots, k-L\}} \mathcal{Y}\}$.

After observing the system state S_k , the decision maker can dispatch vehicles and replenish retailers with inventory. Every decision $x_k \in \mathcal{X}(S_k)$ consists of a routing plan $\mathcal{R}_k = \{R_k^1, \dots, R_k^V\}$, where we omit dependency on x_k, S_k in our notation. Each R_k^v consists of a set of retailers visited by vehicle $v \in \mathcal{V}$, or equals \emptyset . We visit each retailer at most once per period.

Associated with the routing plan, we consider the replenishment plan $\mathcal{U}_k = \{U_k^1, \dots, U_k^N\}$, denoting the amount of inventory being replenished for each retailer. We ensure that the maximum inventory capacity is respected ($I_k^i + U_k^i \leq I^{\max}$) and that the vehicle capacity is respected ($\sum_{i \in R_k^v} U_k^i \leq Q$). We finally impose that $U_k^i = 0 \forall i \in \mathcal{N} \setminus R_k$, as a retailer can only be replenished if it is visited. Formally, the decision space can thus be formulated as:

$$\mathcal{X}(S_k) := \left\{ (\mathcal{R}_k, \mathcal{U}_k) \left| \begin{array}{l} \mathcal{R}_k \text{ partitions a subset of } \mathcal{N} \\ I_k^i + U_k^i \leq I^{\max} \quad \forall i \in \mathcal{N} \\ \sum_{i \in R_k^v} U_k^i \leq Q \quad \forall v \in \mathcal{V} \\ U_k^i = 0 \quad \forall i \in \mathcal{N} \setminus R_k \\ U_k^i \geq 0 \quad \forall i \in \mathcal{N} \end{array} \right. \right\} \quad (1)$$

The exogenous information arriving after decision epoch k is generally denoted by W_{k+1} but is independent of the action x_k in our setting. It consists of the demand observations in period k denoted by \tilde{y}_k^i for each retailer i .

We transition to a new state S_{k+1} via a two-step transition encapsulated by the transition function $S^M(S_k, x_k, W_{k+1})$. First, we apply the replenishment plan of action x_k . The direct cost of decision x_k is the transportation cost $\mathbb{T}(S_k, x_k) := \sum_{v \in \mathcal{V}} \alpha \cdot d(R_k^v)$, where α is a nonnegative scaling parameter and $d(R_k^v)$ denotes the distance of the shortest vehicle route among the retailers in R_k^v , which can be obtained exactly by solving a Traveling Salesman Problem. The post-decision inventory levels at each retailer equal $I_k^i + U_k^i$ for all $i \in \mathcal{N}$. After this, we incur the retailer demand \tilde{y}_k^i at each retailer i , and incur the inventory costs

$$\mathbb{I}(S_k, x_k) := \sum_{i \in \mathcal{N}} (h \max\{0, I_k^i + U_k^i - \tilde{y}_k^i\} - e \min\{I_k^i + U_k^i - \tilde{y}_k^i, 0\}), \quad (2)$$

where h is the per unit holding cost, and e is the per unit backorder cost. We define $C(S_k, x_k) := \mathbb{T}(S_k, x_k) + \mathbb{I}(S_k, x_k)$. Then $I_{k+1}^i = I_k^i + U_k^i - \tilde{y}_k^i$ and $\tilde{Y}_{:k+1}^i = (\tilde{Y}_{:k}^i \setminus \{\tilde{y}_{k-L}^i\}) \cup \{\tilde{y}_k^i\}$ for each retailer i , so that $S_{k+1} = (\mathcal{I}_{k+1}, \tilde{\mathcal{Y}}_{:k+1})$

The goal of the data-driven online inventory routing problem is to find a policy $\pi \in \Pi$ and a decision rule $X^\pi : \mathcal{S} \rightarrow \mathcal{X}(S_k)$ to minimize its total expected future discounted cost:

$$\min_{\pi \in \Pi} \mathbb{E} \left[\sum_{k \in \mathcal{K}} \gamma^k C(S_k, X^\pi(S_k)) \mid S_0 \right], \quad (3)$$

where S_0 is the initial system state, $S_{k+1} = S^M(S_k, X^\pi(S_k), W_{k+1})$ and $\gamma > 0$ is a discount factor.

4. Scenario Predict-then-Optimize

The difficulty of solving Equation (3) is due to the three curses of dimensionality in states, decisions, and transitions. Optimal decisions can only be obtained if each decision's future expected cost is known,

commonly known to be computationally intractable. However, if a reliable description of future retailer demand can be obtained, and can be translated into a set of future demand scenarios, stochastic programming can help to determine an approximate decision that minimizes the expected cost over a smaller, finite future horizon.

In this section, we detail our Scenario Predict-then-Optimize (ScOP) approach that leverages stochastic programming in combination with data-driven future demand scenarios. We first provide a high-level overview of the approach, after which we detail the *scenario-predict* step and the *scenario-optimize* step.

4.1. General Overview of ScenPO

A graphical overview of ScenPO is given in Figure 1. The inventory state transition in our data-driven online inventory routing problem equals $I_{k+1}^i = I_k^i + U_k^i - \tilde{y}_k^i$. The (infinite) support of all future demand realizations equals $\{\times_{i \in \mathcal{N}} \{0, \dots, O\}\}^\infty$. ScenPO considers a narrowed set of future demand realizations at each decision epoch k for each retailer i denoted by Ω_k . Here, $\omega_k \in \Omega_k$ describes the ℓ future demand realization predictions $\hat{Y}_{k:}^{i\omega_k} = \{\hat{y}_{k,k}^{i\omega_k}, \hat{y}_{k,k+1}^{i\omega_k}, \dots, \hat{y}_{k,k+\ell-1}^{i\omega_k}\}$ for each retailer i , with a probability of occurring of $p(\omega_k)$. The scenario-predict step creates a finite set Ω_k at each epoch k via a machine-learning-based prediction G with as input the past demand data $\tilde{\mathcal{Y}}_{:k}$, that is $G(\tilde{\mathcal{Y}}_{:k}) = \langle \Omega_k, \mathcal{P}_k \rangle$, where \mathcal{P}_k is a probability measure mapping predictions ω_k to $p(\omega_k)$. The scenario-predict step thus entails finding a suitable machine learning predictor G on past demand observations $\tilde{\mathcal{Y}}_{:k}$.

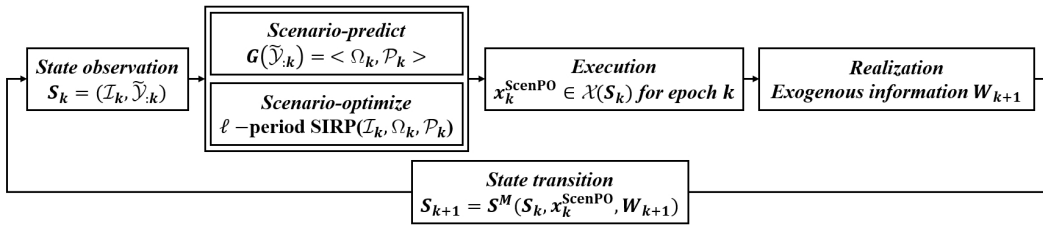


Figure 1 Graphical overview of ScenPO.

Assuming the scenario-predict step of ScenPO returns a set of future demand realizations as described by $\langle \Omega_k, \mathcal{P}_k \rangle$, these predictions must be translated into inventory replenishment and vehicle routing decisions. The scenario-optimize step then exploits two-stage stochastic programming. This two-stage stochastic program is effectively an ℓ -period stochastic inventory routing problem. That is, it determines for the upcoming ℓ periods replenishment and routing decisions that minimize the expected cost over the scenarios Ω_k obtained via predictor G . If ℓ is selected sufficiently large, the future impact of a decision in epoch k can be accurately inferred if the scenarios are a valid representation of the underlying uncertainty (Hvattum et al. 2009). It is important to realize that within the scenario-optimize step, our ScenPO approach considers stage aggregation (Powell 2014). That is, we observe all future demand predictions

within a scenario at once, and do not resort to multi-stage stochastic optimization. Although multi-stage stochastic optimization would give a better estimate of the impact of a decision in epoch k on the future periods' decisions, it is computationally infeasible to solve ℓ -stage stochastic optimization problems at each decision epoch. We illustrate this in Figure 2. We then execute the decisions for epoch k and transition to state S_{k+1} , after which ScenPO restarts.

In summary, ScenPO provides a generic way to deal with MDPs for which the exogenous information exhibits nonstationarity and for which the decision space is of a combinatorial nature, as in the data-driven online inventory routing problem. We refer to the decisions of ScenPO as $x_k^{\text{ScenPO}} \in \mathcal{X}(S_k)$. In the following, we will discuss the details of the scenario-predict and the scenario-optimize step.

4.2. Scenario-Predict Step

The goal is to obtain a data-driven generator of future demand scenarios G . Traditional frameworks for data-driven prediction and optimization often work with point forecasts or, equivalently, mean value prediction. If the optimization is solely based upon a point forecast, it ignores the inherent forecast error of the point forecast. This only works if the point forecast is extremely accurate. However, data-driven online inventory routing and various other applications often have to deal with nonstationary demand patterns subject to exogenous disturbances, which makes it hard to provide reliable and accurate point forecasts.

The scenario-predict step of ScenPO, therefore, does not provide a single-point forecast of future retailer demands. Also, we do not rely on distributional assumptions to generate scenarios. Instead, the scenario-predict step characterizes the shape of future demand realizations by predicting future demand *quantiles*.

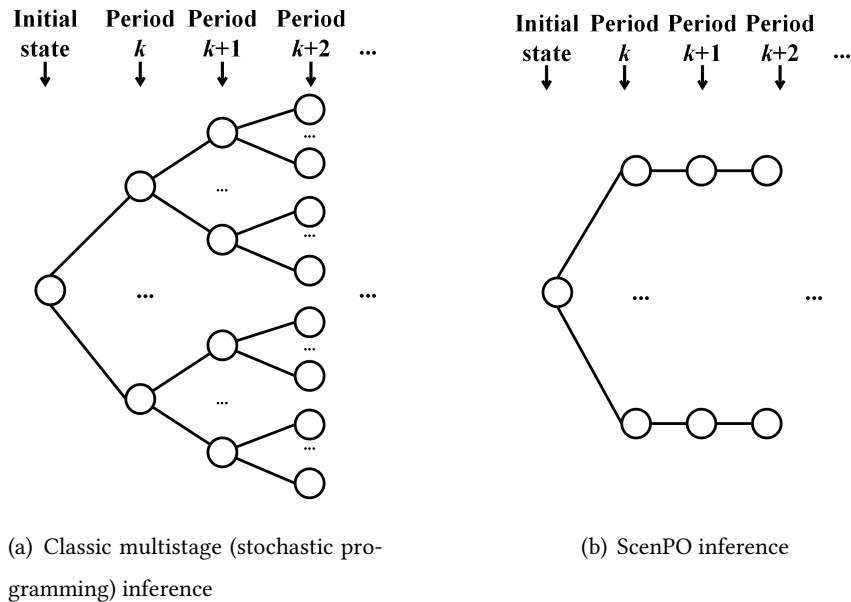


Figure 2 The classic and ScenPO stage and decision structure.

From these demand quantiles, we can then sample uniformly to effectively characterize future retailer demand scenarios without the need for distributional assumptions.

In this section, we first describe the deep learning model we adopt to predict future demand quantiles, the Multi-Horizon Quantile Recurrent Neural Network (MQRNN). Afterward, we discuss how we transform this into a scenario generation method based on the predicted quantiles by the MQRNN. An example of the performance of the MQRNN as eventually employed in our results can be found in Figure 3. Here, the different shades reflect the quantile forecast of future demand.

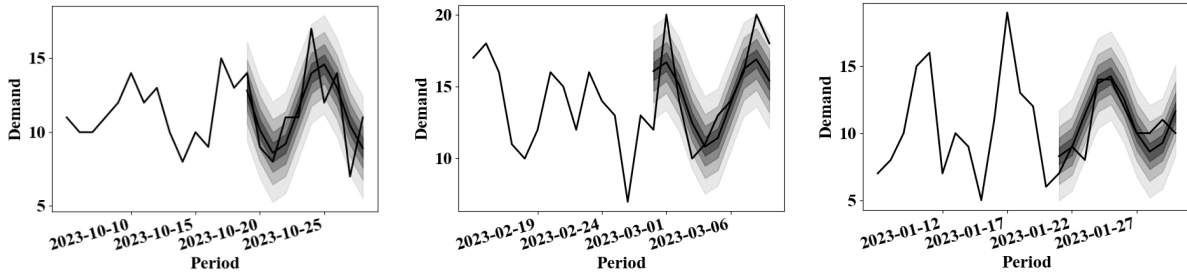


Figure 3 Demand forecast for three example retailers by MQRNN. The different shades of gray represent the predicted quantiles.

We are interested in predicting retailer demand at each of the upcoming ℓ periods. We can only base our prediction on the observation of the last L demand observations $\tilde{\mathcal{Y}}_{:k} = \{\tilde{Y}_{:k}^1, \dots, \tilde{Y}_{:k}^N\}$, where $\tilde{Y}_{:k}^i = \{\tilde{y}_{k-t}^i \mid t \in \{1, 2, \dots, L\}\}$ are the last L periods demands of retailer i . Besides the last demand observations, we consider the periods associated with the demands as features, which can be interpreted as calendar dates or weekdays because demands often correlate with holidays or weekdays. We denote $A_k^l = \{a_{k-t}^l \mid t \in \{1, 2, \dots, L\}\}$ as the dates of history periods and $A_k^f = \{a_{k+t}^f \mid t \in \{0, 1, \dots, \ell - 1\}\}$ as future dates. Using this input, the MQRNN will provide a so-called quantile forecast that gives the conditional quantiles of the target distribution, i.e., the forecasting result of a quantile $b \in \mathcal{B}$ and period k for retailer i , $Y_{k:}^{rib}$, means $\mathbb{P}(Y_{k:}^i \leq Y_{k:}^{rib} \mid \tilde{\mathcal{Y}}_{:k}^i, A_k^l, A_k^f) = b$. Then we have $\{\mathcal{Y}_{k:}^{ib} \mid b \in \mathcal{B}\} = \mathcal{M}(\tilde{\mathcal{Y}}_{:k}, A_k^l, A_k^f)$, where $\mathcal{Y}_{k:}^{ib} = \{Y_{k:}^{rib} \mid i \in \mathcal{N}\}$ and $\mathcal{M}(\cdot)$ is the MQRNN predictor. From this, we can then determine $\langle \Omega_k, \mathcal{P}_k \rangle$.

We now detail the MQRNN structure, which we adopt because of its demonstrated performance in demand forecasting (Wen et al. 2017, Qi et al. 2023). MQRNN exploits the expressiveness and temporal nature of Sequence-to-Sequence Neural Network (Seq2Seq) (Sutskever et al. 2014), mainly including an encoder and decoder part, see Figure 4. MQRNN utilizes the same encoder structure as the classic Seq2Seq framework. The decoder uses a multi-horizon forecast and thus can directly train a model with a multivariate target. There are two kinds of Multi-Layer Perceptron (MLP). They are called a global MLP $m_G(\cdot)$ and a local MLP $m_L(\cdot)$. The global MLP, $(c_{k,k}^i, c_{k,k+1}^i, \dots, c_{k,k+\ell-1}^i, c_{k,a}^i) = m_G(h_{k,k-1}^i, A_k^f)$, summarizes the encoder output ($h_{k,k-1}^i$) plus all future inputs (A_k^f) into two contexts: a series of horizon-specific

contexts $c_{k,k+t}^i$, where $t \in \{0, 1, \dots, \ell - 1\}$, for each of the ℓ future horizons, and a horizon-agnostic context $c_{k,a}^i$, which captures common information. The local MLP applies to each specific horizon, which combines the corresponding future input and the two contexts from the global MLP, then outputs all the required quantiles for that specific future horizon: $(y_{k,k+t}^{ib_1}, y_{k,k+t}^{ib_2}, \dots, y_{k,k+t}^{ib_B}) = m_L(c_{k,k+t}^i, c_{k,a}^i, a_{k+t}^f)$, where $\{b_1, b_2, \dots, b_B\} := \mathcal{B}$. We feed multiple input-target pairs, i.e., ground truth demand realizations $\{\tilde{y}_{\kappa-1}^i, \tilde{y}_{\kappa-2}^i \dots, \tilde{y}_{\kappa-L}^i\} - \{\tilde{y}_{\kappa}^i, \tilde{y}_{\kappa+1}^i \dots, \tilde{y}_{\kappa+\ell-1}^i\}$ for multiple κ and i , to train the encoder-decoder structure. For each input-target pair, the loss function is $\sum_{b \in \mathcal{B}} \sum_{t=0}^{\ell-1} (b(\tilde{y}_{\kappa+t}^i - y_{\kappa,\kappa+t}^{ib})^+ + (1-b)(y_{\kappa,\kappa+t}^{ib} - \tilde{y}_{\kappa+t}^i)^+)$. The model parameters are trained to minimize the total loss of all input-target pairs. The readers are referred to (Wen et al. 2017) for more details.

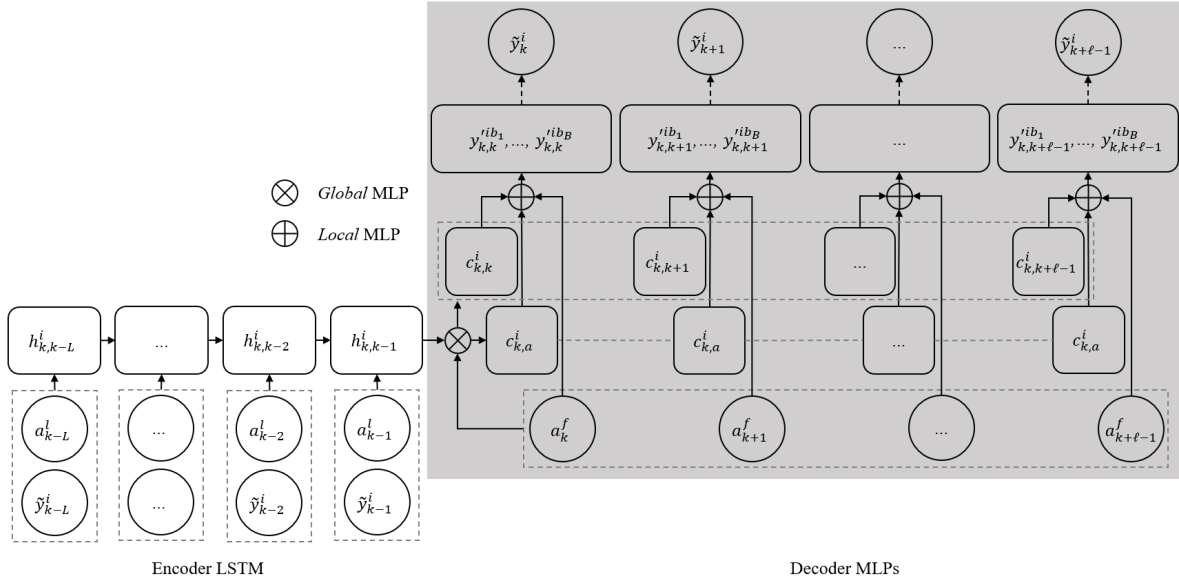


Figure 4 Visualization of the Neural Net Architecture for MQRNN for a single retailer. The dashed boxes flatten nodes into a vector, and dashed lines imply replication. The dashed arrow is the loss, which links network outputs and targets.

Recall that we define a forecasted future demand realization of retailer i in period k as $\hat{Y}_k^{i\omega_k} = \{\hat{y}_{k,k}^{i\omega_k}, \hat{y}_{k,k+1}^{i\omega_k}, \dots, \hat{y}_{k,k+\ell-1}^{i\omega_k}\}$. Here we further define a scenario as $\omega_k = \hat{Y}_k^{i\omega_k} = \{\hat{Y}_k^{i\omega_k} \mid i \in \mathcal{N}\}$. As for the scenario generation, we first include all forecasted quantiles into our scenario set, i.e., $\Omega_k = \{y_{k,t}^{ib} \mid b \in \mathcal{B}\}$. Then, each time we want to generate a new scenario, we first randomly sample a quantile $b_\beta \in \mathcal{B} \setminus \{b_B\}$, then we construct a set of uniform distributions $\{U_{k,k+t}^i \mid i \in \mathcal{N}, t \in \{0, 1, \dots, \ell - 1\}\}$, where $U_{k,k+t}^i$ is bounded by $y_{k,k+t}^{ib_\beta}$ and $y_{k,k+t}^{ib_{\beta+1}}$. Then we generate $\hat{y}_{k,k+t}^{i\omega_k}$ through randomly sampling from distribution $U_{k,k+t}^i$. After we generated all scenarios, we can easily normalize their probabilities to obtain \mathcal{P}_k .

4.3. Scenario-Optimize Step

The scenario-predict step searches for a decision $x_k^{\text{ScenPO}}(S_k) = x_k^{\text{ScenPO}}(\mathcal{I}_k, G(\tilde{\mathcal{Y}}_{:k}))$. It takes as input $G(\tilde{\mathcal{Y}}_{:k})$, and converts this to inventory-replenishment and vehicle-routing decisions by solving an ℓ -period stochastic inventory routing problem.

Recall that \mathcal{N} is the retailer set, and \mathcal{N}^+ is the set of retailers and the warehouse. Then we define the ℓ -period stochastic inventory routing problem on an undirected graph (\mathcal{N}^+, E) , where $E = \{(i, j) : i, j \in \mathcal{N}^+, i \neq j\}$ is the set of edges. Here, c_{ij} denotes the cost of edge (i, j) . We let $\xi^+(i)$ and $\xi^-(i)$ be the subsets of edges starting from i and ending at i , respectively.

We introduce two formulations of the ℓ -period stochastic inventory routing problem called *SS* and *TS*. The *SS* formulation makes the ℓ -period decisions in a single stage, i.e., makes the ℓ -period decisions in epoch k considering different scenarios of demand realizations. Formulation *TS* is in a two-stage fashion: only the decisions in period k are the here-and-now decisions, and the decisions for periods $k+1, k+1, \dots, k+\ell-1$ are wait-and-see decisions, which can be different according to different scenarios realization. That is illustrated in Figure 5.

We first introduce formulation *SS*. We index the decision variables by k to reflect that the system is currently in epoch k . Let binary variable $z_{k,k+t}^{ijv} \in \{0, 1\}$ equal to 1 if vehicle v drives along edge (i, j) at period $k+t$ for $t \in \{0, \dots, \ell-1\}$, and 0 otherwise. Let $u_{k,k+t}^{iv}$ denote the delivery quantity to retailer i by vehicle v in period $k+t$. Note that for integer demand, the delivery quantity will be integer too. Let $\mathcal{T} = \{0, 1, \dots, \ell-1\}$, and let $\hat{I}_{k,k+t}^{i\omega_k}$ denote the inventory at period $k+t$ in scenario $\omega_k \in \Omega_k$. The formulation *SS* is then given by:

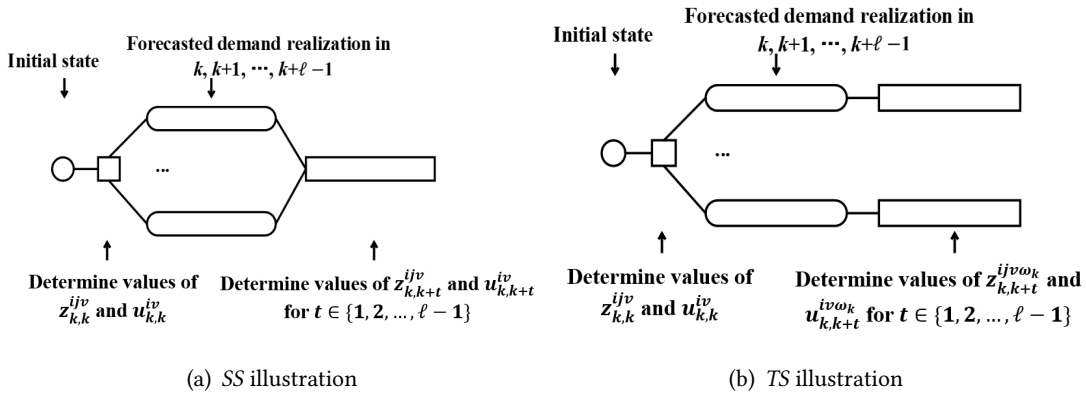


Figure 5 Illustrations for formulations *SS* and *TS*.

$$(SS) \min_{u,z} \sum_{t \in \mathcal{T}} \sum_{(i,j) \in E} \sum_{v \in \mathcal{V}} c_{ij} z_{k,k+t}^{ijv} + \sum_{\omega_k \in \Omega_k} p(\omega_k) \sum_{t \in \mathcal{T}} \sum_{i \in \mathcal{N}} (h(\hat{I}_{k,k+t+1}^{i\omega_k})^+ + e(\hat{I}_{k,k+t+1}^{i\omega_k})^-) \quad (4)$$

$$s.t. \quad \sum_{(i,j) \in \xi^+(0)} z_{k,k+t}^{ijv} = \sum_{(i,j) \in \xi^-(0)} z_{k,k+t}^{ijv} = 1 \quad \forall v \in \mathcal{V}, t \in \mathcal{T}, \quad (5)$$

$$\sum_{(i,j) \in \xi^+(i)} z_{k,k+t}^{ijv} = \sum_{(j,i) \in \xi^-(i)} z_{k,k+t}^{jiv} \quad \forall i \in \mathcal{N}, v \in \mathcal{V}, t \in \mathcal{T}, \quad (6)$$

$$\sum_{v \in \mathcal{V}} \sum_{(i,j) \in \xi^+(i)} z_{k,k+t}^{ijv} \leq 1 \quad \forall i \in \mathcal{N}, t \in \mathcal{T}, \quad (7)$$

$$u_{k,k+t}^{iv} \leq M \sum_{(i,j) \in \xi^+(i)} z_{k,k+t}^{ijv} \quad \forall i \in \mathcal{N}, v \in \mathcal{V}, t \in \mathcal{T}, \quad (8)$$

$$\sum_{i \in \mathcal{N}} u_{k,k+t}^{iv} \leq Q \quad \forall v \in \mathcal{V}, t \in \mathcal{T}, \quad (9)$$

$$u_{k,k+t}^{iv} \leq I^{\max} - \hat{I}_{k,k+t}^{i\omega_k} \quad \forall i \in \mathcal{N}, v \in \mathcal{V}, t \in \mathcal{T}, \omega_k \in \Omega_k, \quad (10)$$

$$\hat{I}_{k,k+t+1}^{i\omega_k} = \hat{I}_{k,k+t}^{i\omega_k} + \sum_{v \in \mathcal{V}} u_{k,k+t}^{iv} - \hat{g}_{k,k+t}^{i\omega_k} \quad \forall i \in \mathcal{N}, t \in \mathcal{T}, \omega_k \in \Omega_k, \quad (11)$$

$$\sum_{i \in S} \sum_{j \in S, j \neq i} z_{k,k+t}^{ijv} \leq |S| - 1 \quad \forall v \in \mathcal{V}, t \in \mathcal{T}, S \subset \mathcal{N}, 2 \leq |S| \leq N, \quad (12)$$

$$z_{k,k+t}^{ijv} \in \{0, 1\} \quad \forall (i, j) \in E, v \in \mathcal{V}, t \in \mathcal{T}, \quad (13)$$

$$u_{k,k+t}^{iv} \geq 0 \quad \forall i \in \mathcal{N}, v \in \mathcal{V}, t \in \mathcal{T}. \quad (14)$$

The Objective Function (4) minimizes the transportation cost and the expected ℓ -period holding and backorder costs under different scenarios. Constraints (5) ensure vehicles start from and end at the warehouse, while Constraints (6) ensure flow conservation. Constraints (7) ensure that each retailer can be visited at most once. Constraints (8) model that a vehicle can only make deliveries to a retailer when it visits the retailer. Constraints (9) and (10) are vehicle capacity and maximum inventory restrictions, respectively. Constraints (11) enforce the inventory flow balance, and Constraints (12) are subtour elimination constraints. Constraints (13) and (14) indicate the variables' domain.

Compared to formulation *SS*, formulation *TS* can make different routing and replenishment decisions for each scenario $\omega_k \in \Omega_k$. For this formulation, we therefore index the variables u and z with a scenario index ω_k .

$$(TS) \min_{u,z} \sum_{\omega_k \in \Omega_k} p(\omega_k) \left(\sum_{t \in \mathcal{T}} \sum_{(i,j) \in E} \sum_{v \in \mathcal{V}} c_{ij} z_{k,k+t}^{ijv\omega_k} + \sum_{t \in \mathcal{T}} \sum_{i \in \mathcal{N}} (h(\hat{I}_{k,k+t+1}^{i\omega_k})^+ + e(\hat{I}_{k,k+t+1}^{i\omega_k})^-) \right), \quad (15)$$

$$s.t. \quad \sum_{(i,j) \in \xi^+(0)} z_{k,k+t}^{ijv\omega_k} = \sum_{(i,j) \in \xi^-(0)} z_{k,k+t}^{ijv\omega_k} = 1 \quad \forall v \in \mathcal{V}, t \in \mathcal{T}, \omega_k \in \Omega_k, \quad (16)$$

$$\sum_{(i,j) \in \xi^+(i)} z_{k,k+t}^{ijv\omega_k} = \sum_{(j,i) \in \xi^-(i)} z_{k,k+t}^{jiv\omega_k} \quad \forall i \in \mathcal{N}, v \in \mathcal{V}, t \in \mathcal{T}, \omega_k \in \Omega_k, \quad (17)$$

$$\sum_{v \in \mathcal{V}} \sum_{(i,j) \in \xi^+(i)} z_{k,k+t}^{ijv\omega_k} \leq 1 \quad \forall i \in \mathcal{N}, t \in \mathcal{T}, \omega_k \in \Omega_k, \quad (18)$$

$$u_{k,k+t}^{iv\omega_k} \leq M \sum_{(i,j) \in \xi^+(i)} z_{k,k+t}^{ijv\omega_k} \quad \forall i \in \mathcal{N}, v \in \mathcal{V}, t \in \mathcal{T}, \omega_k \in \Omega_k, \quad (19)$$

$$\sum_{i \in \mathcal{N}} u_{k,k+t}^{iv\omega_k} \leq Q \quad \forall v \in \mathcal{V}, t \in \mathcal{T}, \omega_k \in \Omega_k, \quad (20)$$

$$u_{k,k+t}^{iv\omega_k} \leq I^{\max} - \hat{I}_{k,k+t}^{i\omega_k} \quad \forall i \in \mathcal{N}, v \in \mathcal{V}, t \in \mathcal{T}, \omega_k \in \Omega_k, \quad (21)$$

$$\hat{I}_{k,k+t+1}^{i\omega_k} = \hat{I}_{k,k+t}^{i\omega_k} + \sum_{v \in \mathcal{V}} u_{k,k+t}^{iv\omega_k} - \hat{y}_{k,k+t}^{i\omega_k} \quad \forall i \in \mathcal{N}, t \in \mathcal{T}, \omega_k \in \Omega_k, \quad (22)$$

$$\sum_{i \in S} \sum_{j \in S, j \neq i} z_{k,k+t}^{ijv\omega_k} \leq |S| - 1 \quad \forall v \in \mathcal{V}, t \in \mathcal{T}, \omega_k \in \Omega_k, S \subset \mathcal{N}, 2 \leq |S| \leq N, \quad (23)$$

$$u_{k,k}^{iv\omega_k} = \bar{u}_{k,k}^{iv} \quad \forall i \in \mathcal{N}, v \in \mathcal{V}, \omega_k \in \Omega_k, \quad (24)$$

$$z_{k,k}^{ijv\omega_k} = \bar{z}_{k,k}^{ijv} \quad \forall (i, j) \in E, v \in \mathcal{V}, \omega_k \in \Omega_k, \quad (25)$$

$$z_{k,k+t}^{ijv\omega_k} \in \{0, 1\} \quad \forall (i, j) \in E, v \in \mathcal{V}, t \in \mathcal{T}, \omega_k \in \Omega_k, \quad (26)$$

$$u_{k,k+t}^{iv\omega_k} \geq 0 \quad \forall i \in \mathcal{N}, v \in \mathcal{V}, t \in \mathcal{T}, \omega_k \in \Omega_k. \quad (27)$$

The Objective Function (15) of *TS* minimizes the expected ℓ -period transportation, holding, and backorder costs. Compared to *SS*, there are two more sets of constraints (24) and (25), which are nonanticipativity constraints to ensure the consistency of decisions among the scenarios in period k .

The optimal solution of *SS* is a feasible solution of *TS*. Formulation *SS* is relatively conservative as we search for a single solution that performs well in all scenarios and do not employ a state-dependent evaluation of decisions in future periods. In contrast, formulation *TS* is relatively optimistic as it allows for state-dependent evaluation of decisions in future periods. However, our state aggregation bases these state-dependent decisions on information that, in practice, is not yet known. Therefore, and because we employ both formulations in a rolling horizon framework, it is unclear which will perform better in practical situations. Among others, we evaluate these differences in Section 6.

After solving either formulation *SS* or *TS*, we let the routing plan $R_k^v = \{i \in \mathcal{N} \mid \sum_{j \in \mathcal{N}^+} z_{k,k}^{ijv} = 1\}$, and the replenishment plan $\mathcal{U}_k = \{\sum_{v \in \mathcal{V}} u_{k,k}^{iv} \mid i \in \mathcal{N}\}$. Then the decision for epoch k can be denoted as $x_k^{\text{ScenPO}}(S_k) = (\mathcal{R}_k, \mathcal{U}_k)$.

5. Algorithms for the Scenario-Optimize Step

Formulation *TS* has second-stage binary variables, making it much more complex to solve than *SS*. Also, *TS* requires the decision in the first period to meet nonanticipativity constraints for all upcoming periods in the aggregated stage. Such formulations clearly cannot be solved by off-the-shelf commercial MIP solvers. Therefore we propose using a Progressive Hedging Algorithm (PHA), which we will outline in Section 5.1. Following that, we present the matheuristic algorithm proposed by Solyalı and Süral (2022) in Section 5.2, which we adopt to solve the *SS* formulation and the subproblems arising in the PHA for the *TS* formulation.

5.1. Progressive Hedging Algorithm (PHA)

The PHA decomposes a multiple-scenario formulation into multiple single-scenario formulations by relaxing the nonanticipativity constraints and then iteratively solving penalized single-scenario formulations, known as subproblems, to reach consensus amongst the first-stage decision variables. Here, consensus

means that they converge to the same value, which is forced via iteratively updating the penalization. Before we detail this, we introduce the one-scenario formulation of TS under scenario ω_k , called $OS(\omega_k)$, as follows:

$$OS(\omega_k) \min_{u,z} \sum_{t \in \mathcal{T}} \sum_{(i,j) \in E} \sum_{v \in \mathcal{V}} c_{ij} z_{k,k+t}^{ijv\omega_k} + \sum_{t \in \mathcal{T}} \sum_{i \in \mathcal{N}} (h(\hat{I}_{k,k+t+1}^{i\omega_k})^+ + e(\hat{I}_{k,k+t+1}^{i\omega_k})^-), \quad (28)$$

$$s.t. \quad \sum_{(i,j) \in \xi^+(0)} z_{k,k+t}^{ijv\omega_k} = \sum_{(i,j) \in \xi^-(0)} z_{k,k+t}^{ijv\omega_k} = 1 \quad \forall v \in \mathcal{V}, t \in \mathcal{T}, \quad (29)$$

$$\sum_{(i,j) \in \xi^+(i)} z_{k,k+t}^{ijv\omega_k} = \sum_{(j,i) \in \xi^-(i)} z_{k,k+t}^{jiv\omega_k} \quad \forall i \in \mathcal{N}, v \in \mathcal{V}, t \in \mathcal{T}, \quad (30)$$

$$\sum_{v \in \mathcal{V}} \sum_{(i,j) \in \xi^+(i)} z_{k,k+t}^{ijv\omega_k} \leq 1 \quad \forall i \in \mathcal{N}, t \in \mathcal{T}, \quad (31)$$

$$u_{k,k+t}^{iv\omega_k} \leq M \sum_{(i,j) \in \xi^+(i)} z_{k,k+t}^{ijv\omega_k} \quad \forall i \in \mathcal{N}, v \in \mathcal{V}, t \in \mathcal{T}, \quad (32)$$

$$\sum_{i \in \mathcal{N}} u_{k,k+t}^{iv\omega_k} \leq Q \quad \forall v \in \mathcal{V}, t \in \mathcal{T}, \quad (33)$$

$$u_{k,k+t}^{iv\omega_k} \leq I^{\max} - \hat{I}_{k,k+t}^{i\omega_k} \quad \forall i \in \mathcal{N}, v \in \mathcal{V}, t \in \mathcal{T}, \quad (34)$$

$$\hat{I}_{k,k+t+1}^{i\omega_k} = \hat{I}_{k,k+t}^{i\omega_k} + \sum_{v \in \mathcal{V}} u_{k,k+t}^{iv\omega_k} - \hat{y}_{k,k+t}^{i\omega_k} \quad \forall i \in \mathcal{N}, t \in \mathcal{T}, \quad (35)$$

$$\sum_{i \in S} \sum_{j \in S, j \neq i} z_{k,k+t}^{ijv\omega_k} \leq |S| - 1 \quad \forall v \in \mathcal{V}, t \in \mathcal{T}, S \subset \mathcal{N}, 2 \leq |S| \leq N, \quad (36)$$

$$z_{k,k+t}^{ijv\omega_k} \in \{0, 1\} \quad \forall (i,j) \in E, v \in \mathcal{V}, t \in \mathcal{T}, \quad (37)$$

$$u_{k,k+t}^{iv\omega_k} \geq 0 \quad \forall i \in \mathcal{N}, v \in \mathcal{V}, t \in \mathcal{T}. \quad (38)$$

Clearly, we cannot just solve each subproblem independently, as it will violate the nonanticipativity constraints. To force nonanticipativity, we can add these constraints with consensus variables to each of the subproblems. Then, we use an augmented Lagrangian relaxation to relax these constraints and add a penalty term in the objective function. Thus, we consider individual scenario subproblems where the objective function can be rewritten as Equation (39), where $\lambda_k^{iv\omega_k}$ denotes Lagrangian multipliers and ρ_k the penalty parameters.

$$f(\omega_k) = \min \sum_{t \in \mathcal{T}} \sum_{(i,j) \in E} \sum_{v \in \mathcal{V}} c_{ij} z_{k,k+t}^{ijv\omega_k} + \sum_{t \in \mathcal{T}} \sum_{i \in \mathcal{N}} (h(\hat{I}_{k,k+t+1}^{i\omega_k})^+ + e(\hat{I}_{k,k+t+1}^{i\omega_k})^-) + \sum_{i \in \mathcal{N}} \sum_{v \in \mathcal{V}} \lambda_k^{iv\omega_k} (u_{k,k}^{iv\omega_k} - \bar{u}_{k,k}^{iv}) + \frac{1}{2} \rho_k \sum_{i \in \mathcal{N}} \sum_{v \in \mathcal{V}} (u_{k,k}^{iv\omega_k} - \bar{u}_{k,k}^{iv})^2, \quad (39)$$

The above objective has a quadratic penalty component containing the integer decision variable. Thus, we adopt the method by Long et al. (2012) to force $u_{k,k}^{iv\omega_k}$ to converge by augmenting the objective function. The objective function can be expressed as Equation (40). Then, Equations (42) and (43) are introduced to linearize the absolute form in Equation (40), and the objective function is rewritten as Equation (41).

$$f(\omega_k) = \min \sum_{t \in \mathcal{T}} \sum_{(i,j) \in E} \sum_{v \in \mathcal{V}} c_{ij} z_{k,k+t}^{ijv\omega_k} + \sum_{t \in \mathcal{T}} \sum_{i \in \mathcal{N}} (h(\hat{I}_{k,k+t+1}^{i\omega_k})^+ + e(\hat{I}_{k,k+t+1}^{i\omega_k})^-) + \sum_{i \in \mathcal{N}} \sum_{v \in \mathcal{V}} \lambda_k^{iv\omega_k} |u_{k,k}^{iv\omega_k} - \bar{u}_{k,k}^{iv}| \quad (40)$$

$$f(\omega_k) = \min \sum_{t \in \mathcal{T}} \sum_{(i,j) \in E} \sum_{v \in \mathcal{V}} c_{ij} z_{k,k+t}^{ijv\omega_k} + \sum_{t \in \mathcal{T}} \sum_{i \in \mathcal{N}} (h(\hat{I}_{k,k+t+1}^{i\omega_k})^+ + e(\hat{I}_{k,k+t+1}^{i\omega_k})^-) + \sum_{i \in \mathcal{N}} \sum_{v \in \mathcal{V}} \lambda_k^{iv\omega_k} (\mu_{k,k}^{iv} + \nu_{k,k}^{iv}) \quad (41)$$

$$s.t. \mu_{k,k}^{iv} - \nu_{k,k}^{iv} = u_{k,k}^{iv\omega_k} - \bar{u}_{k,k}^{iv} \quad \forall i \in \mathcal{N}, v \in \mathcal{V} \quad (42)$$

$$\mu_{k,k}^{iv}, \nu_{k,k}^{iv} \geq 0 \quad \forall i \in \mathcal{N}, v \in \mathcal{V} \quad (43)$$

There are two types of variables, the routing variables \mathbf{z} and the replenishment variables \mathbf{u} . Regarding the consistency of the variables, we have the following result.

PROPOSITION 1 (Consistency). *The consistency of \mathbf{u} among all scenarios is sufficient for the consistency of \mathbf{z} .*

Proof. The only difference among scenarios is the demands faced by retailers. Thus, there is no difference among scenarios once the delivery variable of \mathbf{u} is consistent, which means the optimal solution of \mathbf{z} is consistent. \square

REMARK 1. In the case of degeneracy, we adopt the same seed to solve the subproblems, leading the subproblems to obtain the same routing decision when \mathbf{u} is consistent.

Note that consistency of \mathbf{z} only implies that the maximum total delivery quantity to retailers visited by the same vehicle is consistent. Individual retailer deliveries can differ, so the optimal solution of \mathbf{u} can be inconsistent, given that \mathbf{z} is consistent. According to Proposition 1, once \mathbf{u} is consistent, the optimal solution of \mathbf{z} is consistent. For that reason, we will only enforce nonanticipativity on the \mathbf{u} variables. Furthermore, we observe that small changes in \mathbf{u} will probably not lead to drastic changes to the optimal solution, whereas small changes in \mathbf{z} might lead to drastically different solutions. This observation motivates us to use a myopic policy in our PHA:

MYOPIC POLICY. *During the iterations of PHA, once \mathbf{z} is consistent between two subsequent iterations, we fix \mathbf{z} in all future iterations of PHA.*

As for the consensus variables calculation, parameter updating, and termination criteria, we adopt a similar approach as Hu et al. (2019). The consensus variables are calculated as Equation (44). Equations (45)-(49) show the update of PHA's parameters, where we use superscript of (r) , $r \geq 0$, to represent the parameters under different iterations of PHA and (0) representing the start of the algorithm. After determining the optimal routing decision of \mathbf{z} , we set the parameters update more aggressively, as in Equation

(47), where $\beta^0 = 1$ if \mathbf{z} is inconsistent, and $\beta^0 > 1$ otherwise. The termination criteria are given by Equation (50).

$$\bar{u}_{k,k}^{iv} = \sum_{\omega_k \in \Omega_k} p(\omega_k) u_{k,k}^{iv\omega_k} \quad \forall i \in \mathcal{N}, v \in \mathcal{V}, \quad (44)$$

$$\theta_k^P(r) = \sum_{i \in \mathcal{N}} \sum_{v \in \mathcal{V}} (\bar{u}_{k,k}^{iv(r)} - \bar{u}_{k,k}^{iv(r-1)})^2, \quad (45)$$

$$\theta_k^D(r) = \sum_{i \in \mathcal{N}} \sum_{v \in \mathcal{V}} \sum_{\omega_k \in \Omega_k} (u_{k,k}^{iv\omega_k(r)} - \bar{u}_{k,k}^{iv(r)})^2, \quad (46)$$

$$\rho_k^{(r)} = \begin{cases} \beta^0 \beta^D \rho_k^{(r-1)}, & \text{if } \theta_k^D(r-1) - \theta_k^D(r-2) > 0 \\ \frac{1}{\beta^0 \beta^P} \rho_k^{(r-1)}, & \text{if } \theta_k^P(r-1) - \theta_k^P(r-2) > 0 \\ \rho_k^{(r-1)}, & \text{otherwise} \end{cases} \quad (47)$$

$$\lambda_k^{iv\omega_k(0)} = \rho_k^{(0)} |u_{k,k}^{iv\omega_k(0)} - \bar{u}_{k,k}^{iv(0)}| \quad \forall i \in \mathcal{N}, v \in \mathcal{V}, \omega_k \in \Omega_k, \quad (48)$$

$$\lambda_k^{iv\omega_k(r)} = \rho_k^{(r-1)} |u_{k,k}^{iv\omega_k(r)} - \bar{u}_{k,k}^{iv(r-1)}| + \lambda_k^{iv\omega_k(r-1)} \quad \forall i \in \mathcal{N}, v \in \mathcal{V}, \omega_k \in \Omega_k, \quad (49)$$

$$\sum_{\omega_k \in \Omega_k} p(\omega_k) \left(\sum_{i \in \mathcal{N}} \sum_{v \in \mathcal{V}} |u_{k,k}^{iv\omega_k} - \bar{u}_{k,k}^{iv}| \right) \leq \epsilon. \quad (50)$$

The PHA flow is summarized in Algorithm 1. It iteratively solves penalized subproblems and updates penalty parameters, leading the subproblems under different scenarios to convergence. At the end of every iteration, it will check whether the termination criteria are satisfied. If so, the algorithm will stop, and we can obtain a consensus solution among all scenarios. Note that we also apply the Myopic Policy. Thus, if the routing decision of \mathbf{z} reached consensus during the iterations, we will fix the corresponding routing decisions.

Algorithm 1: The algorithm flow of PHA.

- 1 Initialize: $r \leftarrow 0, \rho_k^{(0)}$.
 - 2 Solve subproblems $OS(\omega_k)$.
 - 3 Calculate consensus variables $\bar{u}_{k,k}^{iv}$ and parameter $\lambda_k^{iv\omega_k(0)}$.
 - 4 **while** not terminate **do**
 - 5 $r \leftarrow r + 1$.
 - 6 Solve subproblems with Objective Function (41).
 - 7 **if** \mathbf{z} is consistent **then**
 - 8 └ Determine the current routing decision as optimal. // Myopic Policy
 - 9 Update consensus variables $\bar{u}_{k,k}^{iv}$, and parameters $\rho_k^{(r)}$ and $\lambda_k^{iv\omega_k(r)}$.
 - 10 **return** $\bar{u}_{k,k}^{iv}$
-

5.2. Matheuristic Algorithm

We adopt the matheuristic algorithm proposed by Solyalı and Süral (2022) to solve $OS(\omega)$ and SS. It is a heuristic algorithm designed for the Deterministic Inventory Routing Problem (DIRP), mainly based on the problem formulation. The DIRP is first formulated as a Mixed Integer Linear Program (MILP), and then three different MILPs of a restricted version of the formulation are constructed. The matheuristic algorithm relies on a sequential solution of the three MILPs, each continuously optimizing the visiting and delivery plan based on the visiting routes constructed through benchmark algorithms for either the Traveling Salesman Problem (TSP) or the Capacitated Vehicle Routing Problem (CVRP). The main idea of this algorithm is avoiding the subtour elimination constraints, which leads to the main solving difficulty. The specific formulations and implementation within PHA are introduced in Appendix A in our online appendix. We refer the reader to Solyalı and Süral (2022) for more details.

5.3. Heuristic Clustering for Large-Scale Problems

Due to the complexity of the data-driven online IRP, even if the scenario decomposition and the matheuristic algorithms are adopted, dealing with large-scale real-life problems in the scenario-optimize step can still be time-consuming. In this subsection, we propose a heuristic clustering algorithm inspired by k-means clustering. Here, we partition retailers into groups with a maximum of N^{\max} retailers at each decision epoch.

In the IRP decision-making process, the transportation plan is determined not only by considering the relative locations of retailers and the warehouse but also the transportation quantity for each retailer. Thus, our clustering algorithm considers the predicted demands besides the distances between retailers. The clustering criterion, defined as the cost of clustering retailer $i \in \mathcal{N}$ into group G , is calculated as (51), where $d(i, G)$ and $d(0, G)$ refer to the geographical distance of retailer i and warehouse 0 to the center of group G , respectively. This equation is basically equivalent to approximating travels with a star centered in the center of group G . r_i estimates the utilization of a vehicle of serving retailer i , as calculated in (52), where ϵ is the decay parameter. The delivery quantity is estimated as the sum of decayed forecasted demand (0.5-quantile) for the future ℓ periods minus the initial inventory. Then, the fractional utilization bounded between 0 and 1 can be calculated as the fraction of delivery quantity and vehicle capacity. $\lceil \sum_{j \in G} r_j + r_i \rceil - \lceil \sum_{j \in G} r_j \rceil$ indicates whether an additional vehicle must be used if retailer i will join group G .

$$c(i, G) = d(i, G) + d(0, G) \left(\lceil \sum_{j \in G} r_j + r_i \rceil - \lceil \sum_{j \in G} r_j \rceil \right), \quad (51)$$

$$r_i = \min \left\{ \max \left\{ \left(\sum_{t=0}^{\ell-1} \epsilon^t y_{k,k+t}^{i/0.5} - I_{k,k}^i \right) / Q, 0 \right\}, 1 \right\}. \quad (52)$$

We apply a standard k-means procedure based on the clustering criteria to partition our retailers into different groups, see for example Sonntag et al. (2023). We stress that this heuristic clustering is performed based on the results of the scenario-predict step (forecasted 0.5-quantile). Thus, the groups will update at each decision epoch instead of determining a fixed group of retailers for the complete planning horizon.

6. Computational Experiments

In this section, we first introduce the configuration of our computational experiments in Section 6.1. We create synthetic data, which allows us to control the “degree of nonstationarity”, i.e., meaning that we can manually impose trends and exogenous disturbances in the data. We conduct numerical experiments to show the performance of our ScenPO in Sections 6.2 and 6.3. We end this section by showing the performance of ScenPO on (large-scale) real-life data at our industry partner in Section 6.4. A sensitivity analysis is provided in Appendix B in our online appendix.

6.1. Experimental Configuration

Our ScenPO is implemented in Python, using SciPy (Virtanen et al. 2020), Scikit-learn (Pedregosa et al. 2011), Torch (Collobert et al. 2011), and PyTorch-Lightning (Falcon and the PyTorch Lightning team 2019). The MILPs of the matheuristic algorithm are solved using CPLEX version 22.1.1.0 (IBM 2022). In several parts, for both the ScenPO and benchmark policies introduced later, we employ a Python TSP Solver to solve the TSP (@FrickTobias 2024) and a Python wrapper for the Hybrid Genetic Search algorithm proposed by Vidal et al. (2012) to solve capacitated vehicle routing problems (@chkwon 2024). The experiments are run on a computer cluster with 2.4 GHz AMD Genoa 9654 (2x) CPU sockets with 2 GB RAM per core.

In the following, we first introduce our data sets. Afterward, we will introduce seven benchmark types to structurally assess all components of ScenPO. We finally discuss our parameter settings.

6.1.1. Synthetic data. We create synthetic instances based on three data patterns: *Trend*, *Random*, and *Both*. For each data pattern, we generate 600 one-year sequences mimicking the demand sequences of 600 retailers, where each sequence is generated as follows. The *Trend* pattern considers a trend and a cycle. We adopt an AR(1) process $v_k = \varphi v_{k-1}$, where for each sequence, φ is randomly sampled from a uniform distribution $U(0.995, 1.01)$ and v_0 is randomly sampled from the uniform distribution $U(5, 7)$. For the cycle factor, we generate value as $w_k = \sin(2\pi/(\hat{a}_k^y/366)) + \sin(2\pi/(\hat{a}_k^w/7))$, where \hat{a}_k^y and \hat{a}_k^w refer to the day of year and day of week, respectively. The final sequence is generated as $v_k + w_k$. The values of the *Random* pattern are randomly sampled from a normal distribution $N(\mu, \sigma^2)$, where for each sequence, μ is sampled from $U(9, 11)$ and σ^2 from $U(2, 4)$. The values of the *Both* pattern are the sum of values generated by the *Trend* and *Random*. We divide the 600 retailers into a training set and a testing set in a ratio of 7:3. The 420 sequences in the training set are fed into prediction models for training, and

the testing set is for constructing instances. For the remaining 180 retailers in the testing set, we use k-means clustering to cluster retailers into 10 different groups based on their locations, generated within the latitude of 50.7-53.4 and longitude 3.5-7.1. Finally, we adjust the groups so that each has 18 retailers. Each group corresponds to an instance. Thus, we have 10 instances of each data pattern, each with 18 retailers.

6.1.2. Benchmarks and ScenPO variants. We consider various benchmarks for solving the data-driven online inventory routing problem. These are:

- First, we consider a *Perfect Information (PI)* solution, which solves at each epoch k an ℓ -period single-scenario inventory routing problem, where the single scenario resembles the true future demands. We will compare each other benchmark as the percentage of the gap closed between an expected value solution and the PI solution.

- Second, we consider the *Expected Value (EV)* solution, where we also solve at each epoch an ℓ -period single-scenario inventory routing problem, but we let the demands of the single scenario be equal to the mean demand at each retailer amongst the last L periods.

- Third, we consider an *Empirical Sampling (EMP)* solution, in which we randomly sample data of the last L periods to create at each epoch a single-scenario inventory routing problem.

- Fourth, we consider a *classic prediction-focused learning paradigm*. Three variants are included, namely where we predict by means of the *MQRNN*, an *LSTM*, or a *Maximum Likelihood Estimation (MLE)*. The single scenario predicted by MQRNN is the 0.5-quantile forecast, $\mathcal{Y}_k^{0.5}$. We train the LSTM to obtain the point forecast of future demands, \mathcal{Y}_k^{LSTM} . For the MLE prediction model, we perform a Chi-square goodness of fit test for normal distribution, exponential distribution, log-normal distribution, Pearson type III distribution, and Weibull minimum distribution on demand sequences to determine the optimal demand distribution and then fit the parameters of the optimal distribution by MLE estimation. At last, the fitted distribution is randomly sampled to generate a single scenario. Summarizing, we consider three prediction-focused learning approaches that predict a single future demand scenario using MQRNN, LSTM, and MLE.

- Fifth, we employ our *Scenario Predict-then-Optimize paradigm with our SS stochastic programming formulation (ScenPO-SS)*. We consider multiple variants of scenario generation, both quantile- and residuals-based. First, we consider scenario generation using the *MLE*, *LSTM*, and *MQRNN* approaches, as they are also used in the prediction-focused learning paradigm introduced above. For LSTM generating multiple scenarios, we use the point forecast of future demands, \mathcal{Y}_k^{LSTM} , as the base value. Then, we sample errors of $\mathcal{E}_k^{\omega_k}$ from a fitted error distribution, which is normal. Demand scenarios are constructed by adding sampled errors to the base value, where different sampled $\mathcal{E}_k^{\omega_k}$ construct different scenarios. For the MLE prediction model, the fitted distribution is randomly sampled multiple times to generate multiple scenarios. The demand scenarios generated by three different models are illustrated in Figure 6. Note, ScenPO-SS

using MQRNN is “our approach” introduced in this paper. In addition, we consider the state-of-the-art data-driven Sample Average Approximation (SAA) proposed by Kannan et al. (2022). They adopt Ordinary Least Squares (OLS) regression to train the prediction model, first used to generate a point prediction. Then, the residuals obtained during training are scaled and added to that point prediction to construct scenarios. They considered three variants of the method, named Empirical Residuals-based SAA (ER-SAA), Jackknife-based SAA (J-SAA), and Jackknife+-based SAA (JP-SAA). We refer readers to Kannan et al. (2022) for more information. We adopt the three approaches as scenario generation benchmarks denoted as *OLS-ER*, *OLS-J*, and *OLS-JP*, respectively. In addition, we present the performance of the residuals-based approach when we obtain a point prediction using *Holt Winters Exponential Smoothing* (called *ES*) or using the *0.5-quantile of the MQRNN* (called *NN*). It is worth noting that since the *ES* approach generates predictions by smoothing historical data, it does not require training prediction models to generate point predictions. Thus, we use training data to only obtain residuals by comparing the ground truth to the forecasted demands. For quantile-based methods, in addition to our ScenPO, we adopt *Quantile Regression* (*QuantReg*) to generate quantiles to evaluate the necessity of deep learning predictors.

- Sixth, we consider our *ScenPO approach using the TS stochastic programming formulation (ScenPO-TS)*, considering MQRNN, LSTM, and MLE as scenario-generation strategies.
- Seventh, we consider the state-of-the-art *decision-focused learning approach proposed by Paulus et al. (2021), named CombOptNet*. It integrates integer programming solvers into neural network architectures as layers capable of learning both the cost terms and the constraints.

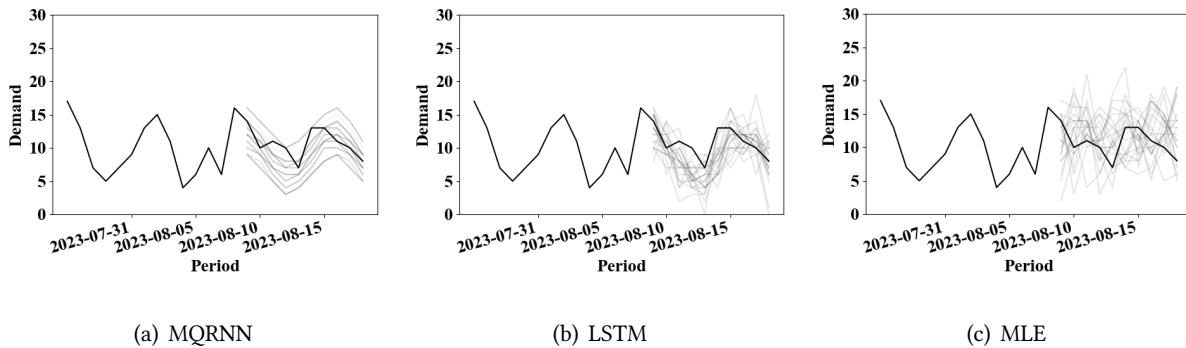


Figure 6 Demand Scenarios generated via different prediction models on the synthetic data of *Both* data pattern.

6.1.3. Parameter values. The per unit holding cost h and per unit backorder cost e are 0.3 and 3, respectively. The scaling parameter α of transportation cost is 0.05 for the synthetic data and 0.01 for the real-life case studies. We use 20 scenarios in our ScenPO variants. The history demand observation of L is set to 14. The look-ahead parameter ℓ is set as 5, 7, and 10, respectively. Since the MQRNN directly outputs the ℓ period prediction, we need to train separately for the different values of ℓ . Thus, we train

three MQRNN predictors for $\ell = 5$, $\ell = 7$, and $\ell = 10$. LSTM adopts a recursive strategy to generate multi-horizon forecasts, i.e., we train one model to predict a one-step-ahead estimate, then iteratively feed this estimate back as the ground truth to forecast longer periods.

We consider a finite time horizon of 30 periods (or epochs) to evaluate the performance of all the methods. The quantiles forecasted by MQRNN and QuantReg are set as $\mathcal{B} = \{0.1, 0.2, \dots, 0.9\}$. The PHA parameters are set as $\beta_D = 1.05$, $\beta_P = 1.05$, $\rho^{(0)} = 0.001$, and $\epsilon = 0.1$. As we evaluate over 30 decision epochs, we set the discount factor to one for simplicity. We set a time limit of 900 seconds for solving the MILPs of the PI, EV, EMP, and prediction-focused learning approaches. For the SS formulation, we consider a time limit per solved MILP of 1800 seconds, considering the complexity of the formulation. For the TS formulation, we set a small time limit of 60 seconds for each MILP in each iteration because we employ PHA to solve it, which requires many more MILP evaluations. We also adopt aggressive PHA convergence parameters to obtain fair comparisons between SS and TS computationally. All approaches run on the server with a single core, except ScenPO-TS, which runs on 10 cores so that we can solve the subproblems in parallel using the threading module (Python Software Foundation 2024). We set the number of threads invoked by CPLEX equal to one.

6.2. Benchmarking ScenPO

In this subsection, we provide a comparison against (a subset of) the seven alternative approaches for solving the data-driven online inventory routing problem. We compare all approaches except the impact of quantile versus residuals-based scenario generation within ScenPO-SS. Those results are presented separately in Section 6.3. The results of CombOptNet are presented in Table A10 in Appendix C in our online appendix as this benchmark approach can only solve small instances due to computational limitations.

We present average performances over five instances, and we vary the number of retailers, the look-ahead parameter ℓ , and the data patterns. A graphical visualization of all the instances, of which details are provided in Tables A4-A6, A11, and A12 in Appendix C in the online appendix, is provided in Figure 7. Here, we present solely the savings of all methods and arrange all the instances horizontally. Savings means the percentage of the gap between the EV and PI approach being closed by that specific method. The instances are numbered as follows: Instances 1-9 correspond to the *Random* data pattern, Instances 10-18 correspond to the *Trend* data pattern, Instances 19-27 correspond to the *Both* data pattern. The remaining are real-life instances Inst-1 and Inst-2, of which we provide a detailed performance separately in Section 6.4. Within each data pattern, the instances are numbered as the increase of the number of retailers and ℓ . For example, Instance 1, Instance 2, and Instance 3 consider five retailers and $\ell = 5$, $\ell = 7$, and $\ell = 10$, respectively. Then Instance 4, Instance 5, and Instance 6 consider seven retailers with $\ell = 5$, $\ell = 7$, and $\ell = 10$, etc. Through the figure, we consistently observe that ScenPO-SS using MQRNN outperforms all other methods. The methods PI, EV, EMP, and the prediction-focused learning methods consider only a single

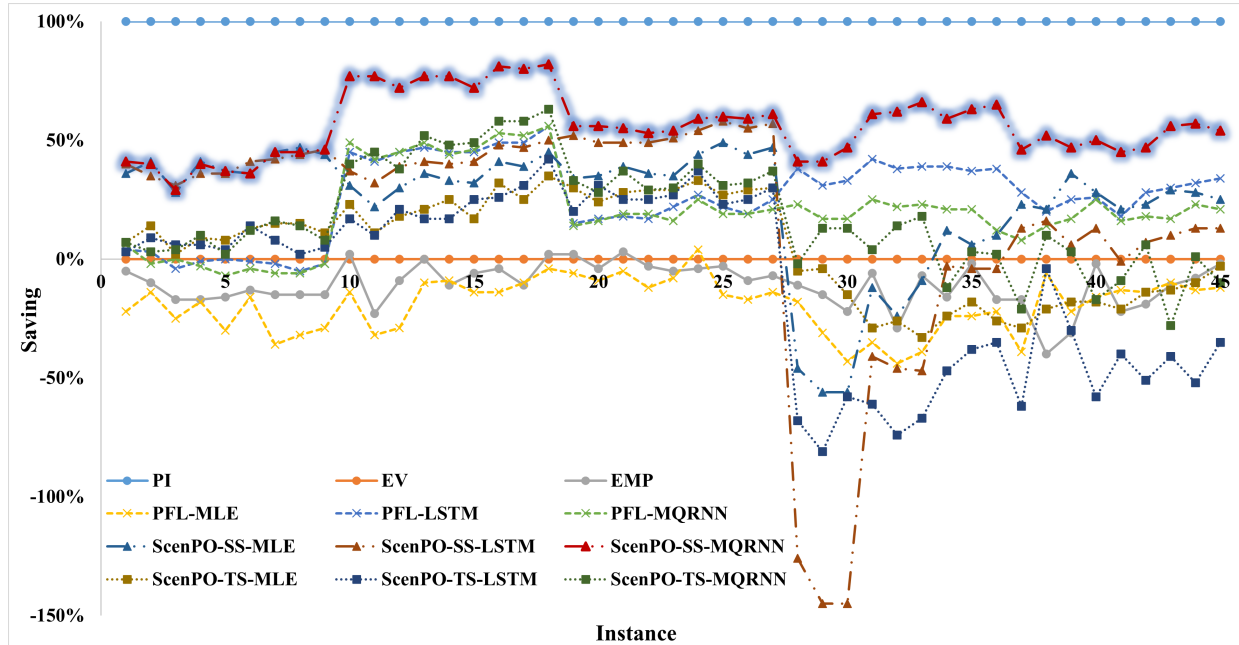


Figure 7 Graphical visualization of all experimental results. The naming of each method refers to the name used in Table 1.

scenario when making decisions. These methods are the fastest to solve, with the average computation time per decision epoch being 705.44s. The ScenPO-SS method takes more time than the single scenario methods, with an average computation time of 1915.11s. The ScenPO-TS method solves formulation *TS* using our PHA algorithm has a computation time of on average 5550.11s.

To further study the detailed differences between the performance of all approaches, we present the results of the instance with ten retailers and the look-ahead length $\ell = 10$ in Table 1, for each of the three data patterns. In Table 1, the row “Cost” refers to the total cost over the 30 periods of each approach. The row “ Δ Cost” is the extra cost compared to the PI approach, and “Saving” means the percentage of the gap between the EV and PI approach being closed. The row “MSE” is the mean-square error of the used prediction. The row “Service” indicates a service level, calculated as the number of directly satisfied demands among all retailers and periods divided by the total demands among all retailers and periods. Finally, the row “Time (s)” is the average computational time for each period in seconds.

Several observations stand out. First, among the three prediction models, MQRNN performs best, and MLE performs worst. The MLE prediction has the lowest saving, with a -15.67% saving on average in prediction-focused learning (implying a worse performance than the EV solution), 45.33% in ScenPO-SS, and 25.33% in ScenPO-TS. The reason is that this model follows the assumption that the distribution is the same in each period and does not consider the trend and cycle changes in demand. That reveals the shortcomings of straightforward distributional assumptions. The LSTM and MQRNN predictions perform

Table 1 Detailed numerical results of ScenPO and the proposed benchmarks for a 10-retailer system.

		PI	EV	EMP	Prediction-Focused Learning			ScenPO-SS			ScenPO-TS		
					MLE	LSTM	MQRNN	MLE	LSTM	MQRNN	MLE	LSTM	MQRNN
<i>Random</i>	Cost	1287	2339	2502	2646	2360	2356	1871	1852	1853	2223	2289	2254
	Δ Cost	0	1053	1216	1360	1073	1069	585	566	567	937	1003	967
	Saving	100%	0%	-15%	-29%	-2%	-2%	44%	46%	46%	11%	5%	8%
	MSE	0	275	570	622	290	284						
	Service	100%	70%	72%	70%	68%	68%	90%	89%	88%	74%	68%	72%
	Time (s)	805	813	810	161	825	814	1961	1965	1741	6482	6382	5666
<i>Trend</i>	Cost	1174	2087	2071	2126	1579	1579	1673	1628	1339	1765	1705	1513
	Δ Cost	0	914	897	952	405	405	499	454	166	591	531	339
	Saving	100%	0%	2%	-4%	56%	56%	45%	50%	82%	35%	42%	63%
	MSE	0	168	377	466	19	20						
	Service	100%	70%	77%	78%	66%	65%	95%	62%	84%	84%	65%	70%
	Time (s)	741	762	784	158	762	756	1925	1945	1689	6085	4214	3822
<i>Both</i>	Cost	1396	2606	2689	2778	2298	2350	2036	1918	1873	2240	2245	2164
	Δ Cost	0	1210	1293	1382	902	954	640	522	477	844	849	768
	Saving	100%	0%	-7%	-14%	25%	21%	47%	57%	61%	30%	30%	37%
	MSE	0	319	738	815	177	194						
	Service	100%	67%	74%	73%	70%	67%	94%	87%	88%	83%	70%	74%
	Time (s)	834	926	863	170	856	858	2072	2059	1879	6104	5901	5295

similarly in the prediction-focused learning approach, with average savings of 26.33% and 25.00%, respectively. In ScenPO-SS, due to the difference in the scenario generation methods, the MQRNN prediction outperforms the LSTM prediction with a 63.00% saving, while the average saving of LSTM is 51.00%. In ScenPO-TS, the average savings of MQRNN and LSTM are 36.00% and 25.67%, respectively. The relatively good performance of MQRNN lies in generating scenarios through forecasted quantiles, which is more robust, while LSTM generates scenarios through base values and error distributions.

The second main observation is that ScenPO-SS outperforms all other benchmarks, including ScenPO-TS, with an average saving of 63.00%. Since MQRNN performs best, we only consider this prediction model in the following analysis. Compared to the EV benchmark, EMP has an average saving of -6.67%. The saving of ScenPO-SS is 63.00% on average. In contrast, the average saving of prediction-focused learning, which represents the traditional prediction-focused learning data-driven approach, is only 25.00%. This shows that ScenPO is a robust alternative that efficiently handles nonstationary data. Relatively surprising, ScenPO-TS does not outperform ScenPO-SS. We will analyze this in more detail later.

Thirdly, ScenPO has the largest improvement under the *Trend* pattern and lowest under the *Random* pattern. This is directly explained by the fact that the *Trend* pattern is the most straightforward to predict. What is also interesting is that the prediction models perform relatively differently among the different data patterns. Focussing on the ScenPO-SS approach, we observe that in the *Trend* pattern, MQRNN outperforms LSTM, having an 82% saving, and LSTM outperforms MLE with a 50% saving compared to a 45% saving. In the *Both* pattern, a similar performance is visible, where the savings of MQRNN, LSTM, and MLE are 61%, 57%, and 47%, respectively. However, the gaps are slightly reduced compared to the *Trend* pattern. In the *Random* pattern, the performance of all models reduces to be similar, with savings of 44%, 46%, and 46% for MLE, LSTM, and MQRNN, respectively. Finally, we noticed that ScenPO-TS does not perform well. One possible reason is the complexity of the model and the need to use PHA; without

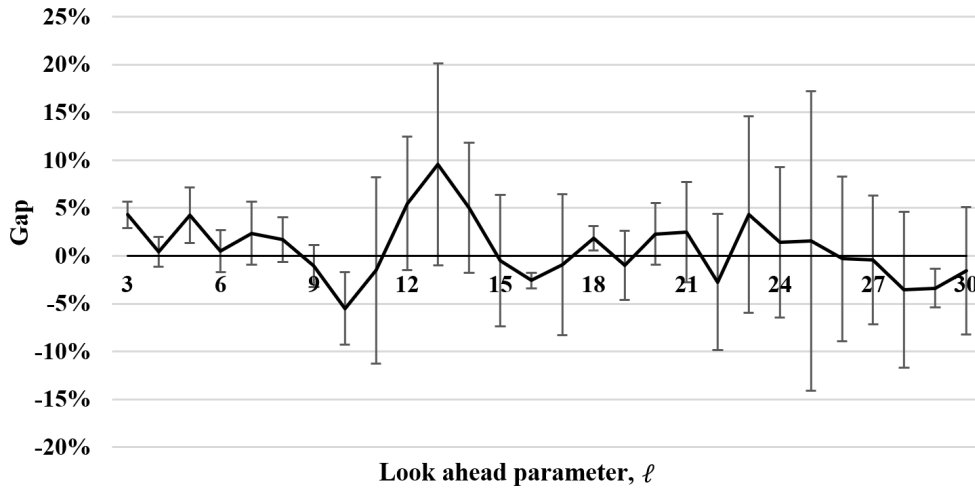


Figure 8 The relative cost comparison of ScenPO-SS compared to ScenPO-TS over different look-ahead lengths ℓ .

that, the models are computationally impossible to solve. Because we need many iterations, we set a one-minute time limit and more aggressive convergence parameters to compress the solution time. To further investigate this, we employ a simple experiment considering the ScenPO-TS and ScenPO-SS approaches for a single retailer setting and vary the value of ℓ . We set a time limit of 1800s. The experiments are on three instances, and the resulting cost over 30 periods within a rolling horizon setting, for varying levels of ℓ , is given in Figure 8, where Gap is calculated as $\frac{\text{Cost}^{TS} - \text{Cost}^{SS}}{\text{Cost}^{SS}}$. We see no clear benefit on either side. ScenPO-SS and ScenPO-TS perform similarly. Future research might want to focus on even more tailored heuristic approaches to solve the ℓ -period stochastic inventory routing problems to see if the ScenPO-TS approach can outperform the ScenPO-SS approach.

6.3. Benchmarking Scenario-Generation Approaches within ScenPO

To further evaluate the value of scenario generation, we conduct numerical experiments considering different scenario generation benchmarks. We compare various residuals- and quantile-based approaches that can be used within ScenPO to create scenarios in the scenario-generate step. For the scenario-optimize step we use the SS stochastic programming formulation.

We provide a graphical visualization of the performance of all approaches among all the instances in Figure 9, similarly as in Figure 7. We observe that the “less predictable” the data becomes, the more noticeably the performance benefit of our ScenPO becomes (the blue-shaded red line). Indeed, on the real-life instances (corresponding to Instances 28 and higher in Figure 9), our ScenPO approach utilizing MQRNN to generate scenarios outperforms the other scenario-generation variants. We analyze and describe this performance on the real-life instances in Section 6.4.

We further study detailed performances of the residuals-based and quantile-based scenario generation strategies within ScenPO-SS by focusing on the 10-retailer system with $\ell = 10$. The results are listed in

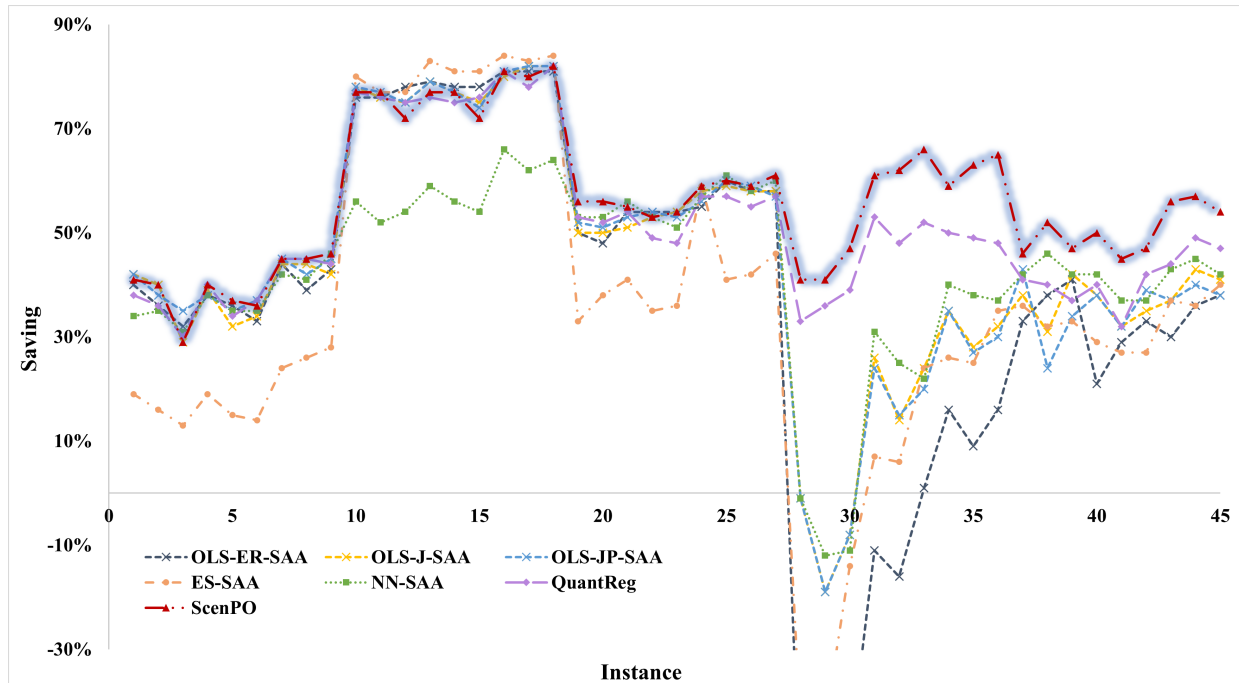


Figure 9 Graphical visualization of the performance of various quantile- and residuals-based scenario generation methods within ScenPO-SS. The naming of each method refers to the name used in Table 2.

Table 2, where the “ScenPO” column refers to our ScenPO-SS approach with MQRNN as the predictor. Note that all columns, except the PI and EV that serve as a reference, are also ScenPO-SS variants but with different scenario-generation approaches. All other results can be found in Tables A7-A9 in Appendix C in our online appendix.

We obtain the following insights. First, the approaches with simple regression methods as predictors (OLS-ER, OLS-J, OLS-JP, and QuantReg) perform well when the data pattern is clear, that is, under the *Trend* dataset. In such cases, these scenario generation methods perform the same as our ScenPO, which has an 82% saving. And among the three methods Kannan et al. (2022) proposed, the OLS-ER method performs slightly worse than the other two methods. The exponential smoothing method performs best, achieving 84% average saving. Second, the different scenario generation methods, except ES, perform similarly when the data pattern has no pattern, that is, under the *Random* dataset. ES performs bad when the data pattern is not clear. Third, when the data pattern is complex, such as under the *Both* dataset, the benchmarks with deep learning-based predictors perform slightly better than simple regression methods.

Our ScenPO performs well under all datasets and slightly outperforms other benchmarks on our synthetic data in general, with an average of 63.00%, while the best-performance residuals-based method (OLS-JP) has an average saving of 61.33%, and QuantReg has an average saving of 61.00%. As for the computation time, different benchmarks perform similarly, with quantile-based methods taking an average of 1779.5s, slightly faster than residuals-based methods taking 1923.27s on average.

Table 2 Comparison of the various quantile- and residuals-based scenario generation approaches within ScenPO for a 10-retailer system.

		PI	EV	residuals-based				quantile-based		
				OLS-ER	OLS-J	OLS-JP	ES	NN	QuantReg	ScenPO
<i>Random</i>	Cost	1287	2339	1889	1893	1867	2041	1852	1872	1853
	ΔCost	0	1053	603	606	580	754	566	586	567
	Saving	100%	0%	43%	42%	45%	28%	46%	44%	46%
	Service	100%	70%	91%	91%	92%	93%	90%	89%	88%
	Time (s)	805	813	1900	1920	1931	1673	1906	1784	1741
<i>Trend</i>	Cost	1174	2087	1346	1342	1340	1321	1504	1336	1339
	ΔCost	0	914	172	168	166	148	330	162	166
	Saving	100%	0%	81%	82%	82%	84%	64%	82%	82%
	Service	100%	70%	85%	83%	85%	88%	72%	83%	84%
	Time (s)	741	762	1860	1901	1902	1891	1821	1691	1689
<i>Both</i>	Cost	1396	2606	1908	1901	1916	2055	1875	1917	1873
	ΔCost	0	1210	512	505	520	659	479	521	477
	Saving	100%	0%	58%	58%	57%	46%	60%	57%	61%
	Service	100%	67%	89%	89%	89%	90%	88%	86%	88%
	Time (s)	834	926	2084	2051	2067	1845	2097	1893	1879

6.4. Real-life Data Experiments

In this subsection, we apply our approaches to real data concerning aftermarket spare parts demand data from SAIC Volkswagen Automotive Co., Ltd. in China in 2020. The transportation and replenishment for retailers in automotive aftermarket content generally refers to the inventory management and transportation from the original equipment manufacturer (SAIC Volkswagen) to retailers or repair shops (hereafter collectively referred to as retailers). We collect the daily order data from retailers to SAIC Volkswagen to estimate the demands faced by retailers. Currently, SAIC Volkswagen has taken the initiative to establish a real-time inventory information-sharing system with retailers. Our work will be a trusty reference for SAIC Volkswagen to promote their future vendor-manged inventory paradigm. Similar as in Gaur and Fisher (2004), we aggregate the demands of multiple spare parts into one according to volume. We divide SAIC Volkswagen’s 1,000 retailers nationwide into a training set and a testing set according to a 70%-30% principle and construct two instances for experiments using a subset of geographically close retailers in the testing set.

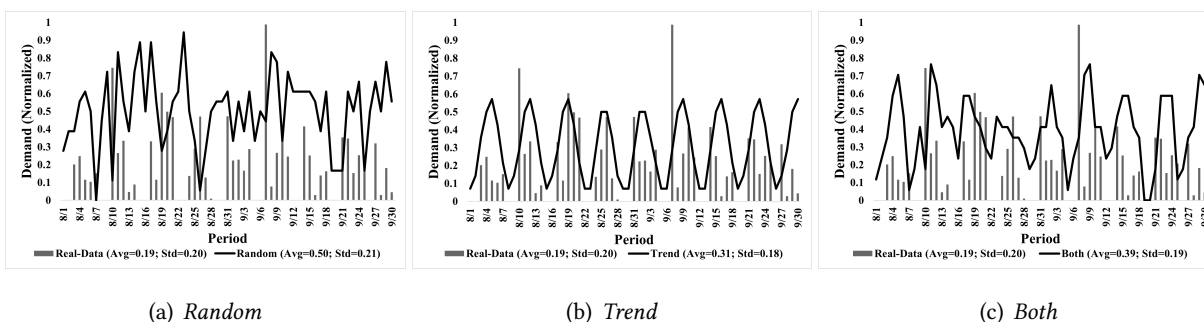


Figure 10 Comparison of real data with synthetic data. Note, these are not forecasted demand versus actual demands, but solely a visualisation of how real-life demand differs from our synthetic data.

Table 3 Real-data experiments for an instance with 10 retailers and $\ell = 10$.

		PI	EV	EMP	Prediction-Focused Learning			ScenPO-SS			ScenPO-TS		
					MLE	LSTM	MQRNN	MLE	LSTM	MQRNN	MLE	LSTM	MQRNN
Inst-1	Cost	585	7697	8917	9296	5027	6846	7006	7971	3097	9571	10188	7579
	Δ Cost	0	7111	8332	8711	4441	6261	6420	7386	2511	8985	9602	6993
	Saving	100%	0%	-17%	-22%	38%	12%	10%	-4%	65%	-26%	-35%	2%
	MSE	0	137	239	376	50	58						
	Service	98%	69%	68%	82%	78%	69%	91%	100%	93%	78%	82%	63%
	Time (s)	87	88	32	19	109	60	50	13	30	5363	5201	3086
	Inst-2	Cost	6411	15103	15285	16140	12130	13320	12915	13981	10395	15337	18126
Δ Cost		0	8692	8874	9729	5719	6908	6504	7570	3984	8926	11715	9525
Saving		100%	0%	-2%	-12%	34%	21%	25%	13%	54%	-3%	-35%	-10%
MSE		0	201	359	410	97	102						
Service		99%	68%	74%	74%	77%	72%	89%	99%	89%	79%	79%	66%
Time (s)		1194	1345	633	233	1348	1265	912	23	774	10487	8931	9936

6.4.1. Example of data used. Figure 10 shows the normalized demands of one random retailer in August and September, which includes the 30 periods we conduct experiments. In the same plots, we also show the data structure used in our synthetic experiments, being it either *Random*, *Trend*, or *Both*. Compared to our synthetic data, we observe that the real-life data has a clear pattern that demands usually occur on weekdays, but the specific demand quantity within each week shows no tendency. We can also observe that real-life data fluctuates greatly with some large orders visible.

6.4.2. Results on real-life data. The results of solving the two real-life instances are shown in Tables 3 and 4, which consists of 10 retailers with $\ell = 10$. Complete results over multiple combinations of number of retailers and value of ℓ can be found in Tables A11-A14 in Appendix C in the online appendix, as well as in the visualization in Figures 7 and 9.

Looking at Table 3, the different benchmarks perform in the real-life case studies similarly to the synthetic data. MQRNN remains the best under the ScenPO-SS approach, and the average savings of MLE, LSTM, and MQRNN are 17.50%, 4.50%, and 59.50%, respectively. Under the prediction-focused learning approach, the average savings are -17.00%, 36.00%, and 16.50%, with LSTM performing better than MQRNN. ScenPO-SS (with MQRNN) still outperforms all other benchmarks with an average savings of 59.50%, while prediction-focused learning (with LSTM) has an average saving of 36.00%, and EMP has an average saving of -9.50%. We note that the performance of LSTM behaves differently. Under ScenPO-SS, the average saving is 4.50%, which is worse than MLE (with an average saving of 17.50%), and the saving is also much lower than LSTM under prediction-focused learning (with an average saving of 36%). The reason lies in the structure of the real-life industry data: fewer patterns can be captured, and thus, more difficult to predict. That can be evidenced by the gaps of "Cost" between different benchmarks and PI. The gaps of ScenPO-SS with MQRNN are 43.98%, 35.28%, and 40.56% for *Random*, *Trend*, and *Both* data patterns, respectively, whereas in real-life industry data, the gaps of these two instances are 429.23% and 62.14%, respectively. As a result, the error distributions fluctuate significantly, leading to poor quality of the scenarios generated by LSTM. That further illustrates the importance of our MQRNN-based scenario

generation method, which is robust enough on different datasets. It also reveals the difficulty of predicting real-life data by point prediction alone. A more powerful multi-scenario approach with robust scenario generation is essential. This is what ScenPO provides.

The computational time to solve the optimization problem in the scenario-optimize step has a similar performance as observed in the synthetic data case, with the approaches considering only a single scenario solving fast, taking on average 534.42s, and the ScenPO-TS method that solves formulation *TS* being slowest with an average computation time of 7167.33s. In contrast, the computation time of ScenPO-SS is 300.33s on average.

Table 4 Further evaluation of different scenario generation approaches for real-date instance with 10 retailers and $\ell = 10$.

		PI	EV	residuals-based					quantile-based	
				OLS-ER	OLS-J	OLS-JP	ES	NN	QuantReg	ScenPO
Inst-1	Cost	585	7697	6551	5455	5551	5240	5091	4251	3097
	Δ Cost	0	7111	5966	4870	4965	4654	4506	3666	2511
	Saving	100%	0%	16%	32%	30%	35%	37%	48%	65%
	Service	98%	69%	93%	93%	92%	93%	94%	88%	93%
	Time (s)	87	88	51	70	73	45	106	23	30
Inst-2	Cost	6411	15103	11805	11514	11826	11667	11485	11015	10395
	Δ Cost	0	8692	5394	5103	5415	5256	5074	4604	3984
	Saving	100%	0%	38%	41%	38%	40%	42%	47%	54%
	Service	99%	68%	92%	88%	89%	90%	91%	85%	89%
	Time (s)	1194	1345	1167	1864	1948	1298	2414	628	774

The performance of scenario generation benchmarks is evaluated in Table 4 for the 10-retailer system with $\ell = 10$. Complete results over multiple parameter combinations can be found in Tables A13 and A14 in Appendix C in the online appendix. Our ScenPO outperforms the other benchmarks, with an average saving of 60.00%, while the best-performance residuals-based approach (NN) has an average saving of 40.00%. This results stand out, as the NN approach takes the 0.5-quantile prediction of the MQRNN, but then samples scenarios via the residuals. It can be interpreted as the residuals-based variant of the method we propose in this paper, as we also use the MQRNN but then sample scenarios uniformly over the quantiles as predicted by the MQRNN.

In addition, we notice that QuantReg also performs competitively in some instances, and the average saving is 48.00%, illustrating the value of the quantile-based scenario generation approach as it also outperforms NN. We also find that taking the deep-learning method as a predictor performs better than simple regression methods, whether for residuals-based or quantile-based methods, showing that deep-learning methods are advantageous to capture the complex correlations for complex real-life data. As for the computation time, the quantile-based methods still have the advantage, with the average time being 363.75s, while the residuals-based methods take 903.60s on average.

Table 5 Real-data experiments of 100-retailer instances.

Instance	ℓ	Item	Prediction-Focused Learning			ScenPO-SS			residuals-based					QuantReg	
			MLE	LSTM	MQRNN	MLE	LSTM	MQRNN	OLS-ER	OLS-J	OLS-JP	ES	NN		
L_Inst_1	5	Cost	116894	78372	85667	97368	119430	65607	84697	78216	77494	89931	75729	71096	
		Service	83%	81%	74%	94%	99%	92%	94%	92%	92%	95%	93%	89%	
		Time (s)	17	183	76	30	11	17	57	154	112	35	186	14	
	7	Cost	118115	78171	87154	96012	120991	66580	92334	82985	83378	88287	78599	69893	
		Service	84%	82%	74%	93%	99%	92%	95%	93%	93%	96%	93%	89%	
		Time (s)	221	736	363	97	14	25	169	562	484	257	1112	25	
	10	Cost	112032	77575	83239	96071	120708	66339	91275	78972	77887	86240	77331	71299	
		Service	85%	82%	75%	94%	99%	91%	94%	92%	92%	94%	93%	88%	
		Time (s)	858	1213	1174	184	25	172	962	1394	1248	832	2248	102	
	L_Inst_2	5	Cost	102252	67518	75885	86293	108049	56473	74867	67826	67874	78692	65914	60960
			Service	83%	80%	72%	94%	99%	92%	95%	94%	93%	97%	94%	89%
			Time (s)	22	47	30	29	10	19	24	27	33	30	101	11
7		Cost	102801	67574	75731	84948	109426	57124	83232	70862	70948	77586	67681	61199	
		Service	83%	81%	73%	94%	99%	92%	95%	94%	94%	97%	94%	88%	
		Time (s)	101	322	137	32	14	41	90	225	228	112	441	28	
10		Cost	101753	67605	73341	86709	109406	56112	81439	68655	68390	74965	68681	61979	
		Service	83%	81%	73%	94%	99%	92%	95%	92%	92%	96%	94%	88%	
		Time (s)	712	989	891	84	19	240	791	1058	990	505	1730	145	

6.4.3. Performance on large-scale real-life data. Finally, since real-life applications always concern many retailers, we also construct two large-scale instances that consider the transportation and replenishment plan for 100 retailers based upon our real-life data from our industry partner. We utilize the heuristic clustering algorithm introduced in Section 5.3, where the maximum number of retailers in each group N^{\max} is set to seven. The results of the large-scale problems are shown in Table 5. The results show that our ScenPO still performs consistently well on large-scale instances. Compared to classic prediction-focused learning with the best-performed predictor (LSTM), our best-performed ScenPO-SS (with predictor MQRNN) decreases the cost by 15.74% on average, and achieves a service level over 90%. Compared to the best-performance residuals-based method (NN), our best-performed ScenPO-SS decreases the cost by 15.18%. QuantReg also performs well, reducing the cost by 8.64% compared to the best-performance residuals-based method. Regarding computation times, ScenPO-SS and QuantReg perform better than other methods and take 69.92s on average. The residuals-based method takes 539.90s on average, while prediction-focused learning approaches take an average of 449.56s.

7. Conclusions

This paper proposes a novel integrated prediction and optimization approach for real-time joint replenishment and distribution via vehicle routing in one-warehouse, multiple-retailer systems, also known as data-driven online inventory routing. Our approach, Scenario Predict-then-Optimize (ScenPO), relies neither on making distributional assumptions for retailer demand nor on single-point forecasts. This contrasts the state-of-the-art that makes such assumptions or works with point forecasts. ScenPO consists of a *scenario-predict* step, utilizing the multi-horizon quantile recurrent neural network that forecasts future retailer demand quantiles from which we sample scenarios. The sampled scenarios are input for

the *scenario-optimize* step of ScenPO, which exploits two-stage stochastic programming to find a solution that minimizes the future expected cost of replenishment and distribution decisions.

In this way, ScenPO can capture (auto)correlation and lumpy retailer demand patterns that typically occur in one warehouse and multiple retailers systems. We show our ScenPO's efficiency based on synthetic data and large-scale real-life data from SAIC Volkswagen Automotive Co., Ltd. We compare ScenPO to empirical sampling techniques, various classical prediction-focused learning approaches, and state-of-the-art data-driven approaches including the decision-focused learning approach, CombOptNet, and various residuals-based sample average approximation approaches for generating scenarios. The results show that our ScenPO outperforms these approaches significantly. It closes 61.60% of the gap between the expected value solution and an oracle solver, whereas the best alternative approach only closes 55.60% on average.

Our ScenPO is general because it leverages neural network-based quantile prediction and stochastic programming. It can easily be tailored to other applications than online inventory routing in which nonstationary demand patterns and online combinatorial optimization are combined. Future research is needed to investigate how to best align the scenario-predict and scenario-optimize steps in other application areas.

Another interesting future research direction is to investigate distributionally robust approaches for application in which only limited data is available. The complexity of the inventory routing problem warrants tailored approaches based upon such distributionally robust approaches, specifically in a dynamic environment.

Another promising avenue for further research is to enrich ScenPO for other variants of online inventory routing problems. For example, one might investigate cyclic delivery patterns to enhance the alignment with other planning processes, consider limited supply availability at the central warehouse, or consider more complex supply chains arising in, for instance, modern city logistics landscapes due to environmental bans of heavy-duty vehicles.

References

- Achamrah FE, Riane F, Limbourg S (2022) Solving inventory routing with transshipment and substitution under dynamic and stochastic demands using genetic algorithm and deep reinforcement learning. *International Journal of Production Research* 60(20):6187–6204.
- Adelman D (2004) A price-directed approach to stochastic inventory/routing. *Operations Research* 52(4):499–514.
- Andersson H, Hoff A, Christiansen M, Hasle G, Løkketangen A (2010) Industrial aspects and literature survey: Combined inventory management and routing. *Computers & Operations Research* 37(9):1515–1536.
- Baty L, Jungel K, Klein PS, Parmentier A, Schiffer M (2024) Combinatorial optimization-enriched machine learning to solve the dynamic vehicle routing problem with time windows. *Transportation Science*.
- Bertazzi L (2008) Analysis of direct shipping policies in an inventory-routing problem with discrete shipping times. *Management Science* 54(4):748–762.
- Cai M, Pipattanasomporn M, Rahman S (2019) Day-ahead building-level load forecasts using deep learning vs. traditional time-series techniques. *Applied Energy* 236:1078–1088.
- Chatfield C (2000) *Time-Series Forecasting* (CRC press).
- Chevillon G (2007) Direct multi-step estimation and forecasting. *Journal of Economic Surveys* 21(4):746–785.
- @chkwon (2024) Pyhygese. URL <https://github.com/chkwon/PyHygese>.
- Cho K, Van Merriënboer B, Gulcehre C, Bahdanau D, Bougares F, Schwenk H, Bengio Y (2014) Learning phrase representations using rnn encoder-decoder for statistical machine translation. *arXiv preprint arXiv:1406.1078*.
- Coelho LC, Cordeau JF, Laporte G (2014a) Heuristics for dynamic and stochastic inventory-routing. *Computers & Operations Research* 52:55–67.
- Coelho LC, Cordeau JF, Laporte G (2014b) Thirty years of inventory routing. *Transportation Science* 48(1):1–19.

- Collobert R, Kavukcuoglu K, Farabet C (2011) Torch7: A matlab-like environment for machine learning. *BigLearn, NIPS Workshop*.
- Crama Y, Rezaei M, Savelsbergh M, Woensel TV (2018) Stochastic inventory routing for perishable products. *Transportation Science* 52(3):526–546.
- Cui Z, Long DZ, Qi J, Zhang L (2023) The inventory routing problem under uncertainty. *Operations Research* 71(1):378–395.
- Dalle G, Baty L, Bouvier L, Parmentier A (2022) Learning with combinatorial optimization layers: a probabilistic approach. *arXiv preprint arXiv:2207.13513*.
- De Gooijer JG, Hyndman RJ (2006) 25 years of time series forecasting. *International Journal of Forecasting* 22(3):443–473.
- Doan HT, Kim M, Song K, Kim H (2024) Locational scenario-based pricing in a bilateral distribution energy market under uncertainty.
- Dong JX, Lee CY, Song DP (2015) Joint service capacity planning and dynamic container routing in shipping network with uncertain demands. *Transportation Research Part B: Methodological* 78:404–421.
- Dong ZS, Xie C, Dai R, Hu S (2022) Resilient route design for collection of material from suppliers with split deliveries and stochastic demands. *Computers & Operations Research* 146:105902.
- Elmachtoub AN, Grigas P (2022) Smart “predict, then optimize”. *Management Science* 68(1):9–26.
- Falcon W, the PyTorch Lightning team (2019) Pytorch lightning. <https://github.com/Lightning-AI/lightning>.
- Ferber A, Wilder B, Dilkina B, Tambe M (2020) Mipaal: Mixed integer program as a layer. *Proceedings of the AAAI Conference on Artificial Intelligence*, volume 34, 1504–1511.
- @FrickTobias (2024) Python tsp solver. URL <https://github.com/fillipe-gsm/python-tsp#python-tsp-solver>.
- Gaur V, Fisher ML (2004) A periodic inventory routing problem at a supermarket chain. *Operations Research* 52(6):813–822.
- Greif T, Bouvier L, Flath CM, Parmentier A, Rohmer SU, Vidal T (2024) Combinatorial optimization and machine learning for dynamic inventory routing. *arXiv preprint arXiv:2402.04463*.
- Hasturk U, Schrottenboer AH, Ursavas E, Roodbergen KJ (2024) Stochastic cyclic inventory routing with supply uncertainty: A case in green-hydrogen logistics. *Transportation Science* 58(2):315–339.
- Hochreiter S, Schmidhuber J (1997) Long short-term memory. *Neural Computation* 9(8):1735–1780.
- Hu S, Han C, Dong ZS, Meng L (2019) A multi-stage stochastic programming model for relief distribution considering the state of road network. *Transportation Research Part B: Methodological* 123:64–87.
- Huber J, Stuckenschmidt H (2020) Daily retail demand forecasting using machine learning with emphasis on calendric special days. *International Journal of Forecasting* 36(4):1420–1438.
- Huh WT, Janakiraman G (2008) (s, S) optimality in joint inventory-pricing control: An alternate approach. *Operations Research* 56(3):783–790.
- Hvattum LM, Løkketangen A (2009) Using scenario trees and progressive hedging for stochastic inventory routing problems. *Journal of Heuristics* 15:527–557.
- Hvattum LM, Løkketangen A, Laporte G (2009) Scenario tree-based heuristics for stochastic inventory-routing problems. *INFORMS Journal on Computing* 21(2):268–285.
- IBM (2022) *IBM ILOG CPLEX Optimization Studio*. IBM, Armonk, NY, URL <https://www.ibm.com/products/ilog-cplex-optimization-studio>, version 22.1.1.0.
- Jaillet P, Bard JF, Huang L, Dror M (2002) Delivery cost approximations for inventory routing problems in a rolling horizon framework. *Transportation Science* 36(3):292–300.
- Jalilvand M, Bashiri M, Nikzad E (2021) An effective progressive hedging algorithm for the two-layers time window assignment vehicle routing problem in a stochastic environment. *Expert Systems with Applications* 165:113877.
- Kannan R, Bayraksan G, Luedtke JR (2022) Data-driven sample average approximation with covariate information. *arXiv preprint arXiv:2207.13554*.
- Keskin M, Branke J, Deineko V, Strauss AK (2023) Dynamic multi-period vehicle routing with routing. *European Journal of Operational Research* 310(1):168–184.
- Kim G, Wu K, Huang E (2015) Optimal inventory control in a multi-period newsvendor problem with non-stationary demand. *Advanced Engineering Informatics* 29(1):139–145.
- Kim M, Park T, Jeong J, Kim H (2023) Stochastic optimization of home energy management system using clustered quantile scenario reduction. *Applied Energy* 349:121555.
- Kleywegt AJ, Nori VS, Savelsbergh MW (2002) The stochastic inventory routing problem with direct deliveries. *Transportation Science* 36(1):94–118.
- Kleywegt AJ, Nori VS, Savelsbergh MW (2004) Dynamic programming approximations for a stochastic inventory routing problem. *Transportation Science* 38(1):42–70.
- Koenker R, Bassett Jr G (1978) Regression quantiles. *Econometrica: journal of the Econometric Society* 33–50.
- Kotary J, Fioretto F, Van Hentenryck P, Wilder B (2021) End-to-end constrained optimization learning: A survey. *arXiv preprint arXiv:2103.16378*.
- Lim B, Zohren S (2021) Time-series forecasting with deep learning: a survey. *Philosophical Transactions of the Royal Society A* 379(2194):20200209.
- Liu H, Grigas P (2022) Online contextual decision-making with a smart predict-then-optimize method. *arXiv preprint arXiv:2206.07316*.
- Long Y, Lee LH, Chew EP (2012) The sample average approximation method for empty container repositioning with uncertainties. *European Journal of Operational Research* 222(1):65–75.
- Mandi J, Guns T (2020) Interior point solving for lp-based prediction+ optimisation. *Advances in Neural Information Processing Systems* 33:7272–7282.
- Mandi J, Kotary J, Berden S, Mulamba M, Bucarey V, Guns T, Fioretto F (2023) Decision-focused learning: Foundations, state of the art, benchmark and future opportunities. *arXiv preprint arXiv:2307.13565*.
- Mandi J, Stuckey PJ, Guns T, et al. (2020) Smart predict-and-optimize for hard combinatorial optimization problems. *Proceedings of the AAAI Conference on Artificial Intelligence*, volume 34, 1603–1610.
- Parmentier A (2021) Learning structured approximations of combinatorial optimization problems. *arXiv preprint arXiv:2107.04323*.
- Parmentier A (2022) Learning to approximate industrial problems by operations research classic problems. *Operations Research* 70(1):606–623.
- Paulus A, Rolínek M, Musil V, Amos B, Martius G (2021) Comboptnet: Fit the right np-hard problem by learning integer programming constraints. *International Conference on Machine Learning*, 8443–8453 (PMLR).
- Pedregosa F, Varoquaux G, Gramfort A, Michel V, Thirion B, Grisel O, Blondel M, Prettenhofer P, Weiss R, Dubourg V, et al. (2011) Scikit-learn: Machine learning in python. *Journal of machine learning research* 12(Oct):2825–2830.
- Powell WB (2014) Clearing the jungle of stochastic optimization. *Bridging Data and Decisions*, 109–137 (Informs).

- Python Software Foundation (2024) *Thread-based parallelism (threading)*. URL <https://docs.python.org/3/library/threading.html>, accessed: 2024-07-09.
- Qi M, Shen ZJ (2022) Integrating prediction/estimation and optimization with applications in operations management. *Tutorials in operations research: emerging and impactful topics in operations*, 36–58 (INFORMS).
- Qi M, Shi Y, Qi Y, Ma C, Yuan R, Wu D, Shen ZJ (2023) A practical end-to-end inventory management model with deep learning. *Management Science* 69(2):759–773.
- Rockafellar RT, Wets RJB (1991) Scenarios and policy aggregation in optimization under uncertainty. *Mathematics of Operations Research* 16(1):119–147.
- Sadana U, Chenreddy A, Delage E, Forel A, Frejinger E, Vidal T (2024) A survey of contextual optimization methods for decision-making under uncertainty. *European Journal of Operational Research*.
- Sahay N, Ierapetritou M (2016) Multienterprise supply chain: Simulation and optimization. *AIChE Journal* 62(9):3392–3403.
- Solyali O, Süral H (2022) An effective matheuristic for the multivehicle inventory routing problem. *Transportation Science* 56(4):1044–1057.
- Song K, Jeong J, Moon JH, Kwon SC, Kim H (2022) Dtrans: Pv power forecasting using delaunay triangulation and transgru. *Sensors* 23(1):144.
- Sonntag DR, Schrottenboer AH, Kiesmüller GP (2023) Stochastic inventory routing with time-based shipment consolidation. *European Journal of Operational Research* 306(3):1186–1201.
- Staudemeyer RC, Morris ER (2019) Understanding lstm—a tutorial into long short-term memory recurrent neural networks. *arXiv preprint arXiv:1909.09586*.
- Sutskever I, Vinyals O, Le QV (2014) Sequence to sequence learning with neural networks. *Advances in Neural Information Processing Systems* 27.
- US Census Bureau (2022) The annual retail trade survey. URL <https://www.census.gov/programs-surveys/arts.html>.
- Vidal T, Crainic TG, Gendreau M, Lahrichi N, Rei W (2012) A hybrid genetic algorithm for multidepot and periodic vehicle routing problems. *Operations Research* 60(3):611–624.
- Virtanen P, Gommers R, Oliphant TE, Haberland M, Reddy T, Cournapeau D, Burovski E, Peterson P, Weckesser W, Bright J, van der Walt SJ, Brett M, Wilson J, Millman KJ, Mayorov N, Nelson ARJ, Jones E, Kern R, Larson E, Carey CJ, Polat İ, Feng Y, Moore EW, VanderPlas J, Laxalde D, Perktold J, Cimrman R, Henriksen I, Quintero EA, Harris CR, Archibald AM, Ribeiro AH, Pedregosa F, van Mulbregt P, SciPy 10 Contributors (2020) SciPy 1.0: Fundamental Algorithms for Scientific Computing in Python. *Nature Methods* 17:261–272, URL <http://dx.doi.org/10.1038/s41592-019-0686-2>.
- Vlastelica M, Paulus A, Musil V, Martius G, Rolínek M (2019) Differentiation of blackbox combinatorial solvers. *arXiv preprint arXiv:1912.02175*.
- Wang Y, Gan D, Sun M, Zhang N, Lu Z, Kang C (2019) Probabilistic individual load forecasting using pinball loss guided lstm. *Applied Energy* 235:10–20.
- Wen R, Torkkola K, Narayanaswamy B, Madeka D (2017) A multi-horizon quantile recurrent forecaster. *arXiv preprint arXiv:1711.11053*.
- Wilder B, Dilkina B, Tambe M (2019) Melding the data-decisions pipeline: Decision-focused learning for combinatorial optimization. *Proceedings of the AAAI Conference on Artificial Intelligence*, volume 33, 1658–1665.
- Xu Y, Bisi A, Dada M (2011) A periodic-review base-stock inventory system with sales rejection. *Operations Research* 59(3):742–753.
- Ye W, You F (2016) A computationally efficient simulation-based optimization method with region-wise surrogate modeling for stochastic inventory management of supply chains with general network structures. *Computers & Chemical Engineering* 87:164–179.

Appendix A: Matheuristic Algorithm

The algorithm follows the following steps:

- Step 1. Solve a TSP over all retailers,
- Step 2. Solve *MILP1*,
- Step 3. Solve a TSP if only one vehicle is enabled or a CVRP else for each $t \in \mathcal{T}$,
- Step 4. Solve *MILP2*,
- Step 5. Solve a TSP for each route in each $t \in \mathcal{T}$,
- Step 6. Solve *MILP3*,
- Step 7. Solve a TSP for each vehicle in each $t \in \mathcal{T}$.

Next, we will introduce the MILPs and the penalized objective functions implemented in the PHA. Here, we omit the notation of ω_k .

Based on the TSP solution, we define $\alpha_k(i)$ and $\beta_k(i)$ as the retailer sets visited after and before retailer i . When $i = 0$ or $j = 0$, $z_{k,k+t}^{ij}$ is an integer variable indicating the visit times to the warehouse. Otherwise, $z_{k,k+t}^{ij}$ is a binary variable indicating whether the corresponding edge is visited. Then, we can formulate the *MILP1* formulation. Compared to *OS*(ω_k), we ignore the vehicle index v in the *MILP1* formulation and construct the vehicle route based on the TSP solution. Thus, the sub-tour elimination constraints are no longer required.

$$(MILP1) \min \sum_{t \in \mathcal{T}} \sum_{(i,j) \in E} c_{ij} z_{k,k+t}^{ij} + \sum_{t \in \mathcal{T}} \sum_{i \in \mathcal{N}} (h(\hat{I}_{k,k+t+1}^i)^+ + e(\hat{I}_{k,k+t+1}^i)^-), \quad (A1)$$

$$s.t. \sum_{(i,j) \in \xi^+(0)} z_{k,k+t}^{ij} = \sum_{(i,j) \in \xi^-(0)} z_{k,k+t}^{ij} = V \quad \forall t \in \mathcal{T}, \quad (A2)$$

$$\sum_{j \in \alpha(i)} z_{k,k+t}^{ij} = \sum_{j \in \beta(i)} z_{k,k+t}^{ij} \quad \forall i \in \mathcal{N}, t \in \mathcal{T}, \quad (A3)$$

$$\sum_{j \in \alpha(i)} z_{k,k+t}^{ij} \leq 1 \quad \forall i \in \mathcal{N}, t \in \mathcal{T}, \quad (A4)$$

$$u_{k,k+t}^i \leq M \sum_{j \in \alpha(i)} z_{k,k+t}^{ij} \quad \forall i \in \mathcal{N}, t \in \mathcal{T}, \quad (A5)$$

$$\sum_{i \in \mathcal{N}} u_{k,k+t}^i \leq Q \sum_{j \in \mathcal{N}} z_{k,k+t}^{0j} \quad \forall t \in \mathcal{T}, \quad (A6)$$

$$u_{k,k+t}^i \leq I^{\max} - \hat{I}_{k,k+t}^i \quad \forall i \in \mathcal{N}, t \in \mathcal{T}, \quad (A7)$$

$$\hat{I}_{k,k+t+1}^i = \hat{I}_{k,k+t}^i + u_{k,k+t}^i - \hat{y}_{k,k+t}^i \quad \forall i \in \mathcal{N}, t \in \mathcal{T}, \quad (A8)$$

$$z_{k,k+t}^{ij} \in \{0, 1\} \quad \forall (i,j) \in E, t \in \mathcal{T}, \quad (A9)$$

$$u_{k,k+t}^i \geq 0 \quad \forall i \in \mathcal{N}, t \in \mathcal{T}. \quad (A10)$$

When implemented in PHA, the penalized objective will be modified as Equation (A11), while constraints (A12) and (A13) are added. The aggregated PHA parameter λ_k^i is calculated as Equation (A14) and (A15).

$$\min \sum_{t \in \mathcal{T}} \sum_{(i,j) \in E} c_{ij} z_{k,k+t}^{ij} + \sum_{t \in \mathcal{T}} \sum_{i \in \mathcal{N}} (h(\hat{I}_{k,k+t+1}^i)^+ + e(\hat{I}_{k,k+t+1}^i)^-) + \sum_{i \in \mathcal{N}} \lambda_k^i (\mu_{k,k}^i + \nu_{k,k}^i), \quad (A11)$$

$$s.t. \mu_{k,k}^i - \nu_{k,k}^i = u_{k,k}^i - \sum_{v \in \mathcal{V}} \bar{u}_{k,k}^{iv} \quad \forall i \in \mathcal{N}, t \in \mathcal{T}, \quad (A12)$$

$$\mu_{k,k}^i, \nu_{k,k}^i \geq 0 \quad \forall i \in \mathcal{N}, t \in \mathcal{T}. \quad (A13)$$

$$\lambda_k^{i(0)} = \rho_k^{(0)} \left| \sum_{v \in \mathcal{V}} u_{k,k}^{iv(0)} - \sum_{v \in \mathcal{V}} \bar{u}_{k,k}^{iv(0)} \right| \quad \forall i \in \mathcal{N}, \quad (\text{A14})$$

$$\lambda_k^{i(r)} = \rho_k^{(r-1)} \left| \sum_{v \in \mathcal{V}} u_{k,k}^{iv(r)} - \sum_{v \in \mathcal{V}} \bar{u}_{k,k}^{iv(r-1)} \right| + \lambda_k^{i(r-1)} \quad \forall i \in \mathcal{N}. \quad (\text{A15})$$

Since *MILP1* only considers the aggregated vehicle capacity constraints, the solution obtained may be unfeasible. Therefore, *MILP2* is constructed to make the solution feasible or to improve it by exchanging retailers among routes. The notations needed are defined as follows.

Table A1 Additional notations for *MILP2*.

Parameters	
$\Gamma_{k,k+t}^{iv}$	driving cost of inserting retailer i to route v in $k+t$
$\Delta_{k,k+t}^{iv}$	driving cost saving of removing retailer i from route v in $k+t$
$a_{k,k+t}^{iv}$	indicator parameter of whether retailer i is visited by route v in $k+t$ in the solution
Decision Variables	
$s_{k,k+t}^{iv}$	binary variable indicating whether retailer i is inserted to route v in $k+t$
$r_{k,k+t}^{iv}$	binary variable indicating whether retailer i is removed from route v in $k+t$

$$(\text{MILP2}) \min \sum_{t \in \mathcal{T}} \sum_{i \in \mathcal{N}} (h(\hat{I}_{k,k+t+1}^i)^+ + e(\hat{I}_{k,k+t+1}^i)^-) + \sum_{t \in \mathcal{T}} \sum_{i \in \mathcal{N}} \sum_{v \in \mathcal{V}} ((1 - a_{k,k+t}^{iv}) \Gamma_{k,k+t}^{iv} s_{k,k+t}^{iv} - a_{k,k+t}^{iv} \Delta_{k,k+t}^{iv} r_{k,k+t}^{iv}), \quad (\text{A16})$$

$$\text{s.t.} \sum_{v \in \mathcal{V}} (a_{k,k+t}^{iv} - a_{k,k+t}^{iv} r_{k,k+t}^{iv} + (1 - a_{k,k+t}^{iv}) s_{k,k+t}^{iv}) \leq 1 \quad \forall i \in \mathcal{N}, t \in \mathcal{T}, \quad (\text{A17})$$

$$u_{k,k+t}^{iv} \leq M(a_{k,k+t}^{iv} - a_{k,k+t}^{iv} r_{k,k+t}^{iv} + (1 - a_{k,k+t}^{iv}) s_{k,k+t}^{iv}) \quad \forall i \in \mathcal{N}, t \in \mathcal{T}, v \in \mathcal{V}, \quad (\text{A18})$$

$$\sum_{i \in \mathcal{N}} u_{k,k+t}^{iv} \leq Q \quad \forall t \in \mathcal{T}, v \in \mathcal{V}, \quad (\text{A19})$$

$$u_{k,k+t}^{iv} \leq I^{\max} - \hat{I}_{k,k+t}^i \quad \forall i \in \mathcal{N}, t \in \mathcal{T}, v \in \mathcal{V}, \quad (\text{A20})$$

$$\hat{I}_{k,k+t+1}^i = \hat{I}_{k,k+t}^i + \sum_{v \in \mathcal{V}} u_{k,k+t}^{iv} - \hat{y}_{k,k+t}^i \quad \forall i \in \mathcal{N}, t \in \mathcal{T}, \quad (\text{A21})$$

$$r_{k,k+t}^{iv} \in \{0, 1\} \quad \forall i \in \mathcal{N}, t \in \mathcal{T}, v \in \mathcal{V}, \quad (\text{A22})$$

$$s_{k,k+t}^{iv} \in \{0, 1\} \quad \forall i \in \mathcal{N}, t \in \mathcal{T}, v \in \mathcal{V}, \quad (\text{A23})$$

$$u_{k,k+t}^{iv} \geq 0 \quad \forall i \in \mathcal{N}, t \in \mathcal{T}, v \in \mathcal{V}. \quad (\text{A24})$$

The objective of *MILP2* in PHA is modified to Equation (A25), with Constraints (A26) and (A27).

$$\min \sum_{t \in \mathcal{T}} \sum_{i \in \mathcal{N}} (h(\hat{I}_{k,k+t+1}^i)^+ + e(\hat{I}_{k,k+t+1}^i)^-) + \sum_{t \in \mathcal{T}} \sum_{i \in \mathcal{N}} \sum_{v \in \mathcal{V}} ((1 - a_{k,k+t}^{iv}) \Gamma_{k,k+t}^{iv} s_{k,k+t}^{iv} - a_{k,k+t}^{iv} \Delta_{k,k+t}^{iv} r_{k,k+t}^{iv}) + \sum_{i \in \mathcal{N}} \sum_{v \in \mathcal{V}} \lambda_k^{iv} (\mu_{k,k}^{iv} + \nu_{k,k}^{iv}), \quad (\text{A25})$$

$$\text{s.t.} \mu_{k,k}^{iv} - \nu_{k,k}^{iv} = u_{k,k+t}^{iv} - \bar{u}_{k,k+t}^{iv} \quad \forall i \in \mathcal{N}, v \in \mathcal{V}, \quad (\text{A26})$$

$$\mu_{k,k}^{iv}, \nu_{k,k}^{iv} \geq 0 \quad \forall i \in \mathcal{N}, v \in \mathcal{V}. \quad (\text{A27})$$

Table A2 Additional notations for MILP3.

Sets	
$\mathcal{V}_{k,k+t}$	set of vehicles used in $k+t$ in the solution of the last step, $\mathcal{V}_{k,k+t} = \{1, 2, \dots, V_{k,k+t}\}$
Parameters	
$\alpha_{k,k+t}^v(i)$	the retailer set visited after retailer i in $k+t$ by route v
$\beta_{k,k+t}^v(i)$	the retailer set visited before retailer i in $k+t$ by route v

Then, formulation MILP3 is further formulated to enhance the solution with the notations listed in Table A2.

$$(MILP3) \min \sum_{t \in \mathcal{T}} \sum_{(i,j) \in E} \sum_{v \in \mathcal{V}_{k,k+t}} c_{ij} z_{k,k+t}^{ijv} + \sum_{t \in \mathcal{T}} \sum_{i \in \mathcal{N}} (h(\hat{I}_{k,k+t+1}^i)^+ + e(\hat{I}_{k,k+t+1}^i)^-), \quad (A28)$$

$$s.t. \sum_{(i,j) \in \xi^+(0)} z_{k,k+t}^{ijv} = \sum_{(i,j) \in \xi^-(0)} z_{k,k+t}^{ijv} = 1 \quad \forall t \in \mathcal{T}, v \in \mathcal{V}_{k,k+t}, \quad (A29)$$

$$\sum_{j \in \alpha_{k,k+t}^v(i)} z_{k,k+t}^{ijv} = \sum_{j \in \beta_{k,k+t}^v(i)} z_{k,k+t}^{ijv} \quad \forall i \in \mathcal{N}, t \in \mathcal{T}, v \in \mathcal{V}_{k,k+t}, \quad (A30)$$

$$\sum_{v \in \mathcal{V}_{k,k+t}} \sum_{j \in \alpha_{k,k+t}^v(i)} z_{k,k+t}^{ijv} \leq 1 \quad \forall i \in \mathcal{N}, t \in \mathcal{T}, \quad (A31)$$

$$u_{k,k+t}^{iv} \leq M \sum_{j \in \alpha_{k,k+t}^v(i)} z_{k,k+t}^{ijv} \quad \forall i \in \mathcal{N}, t \in \mathcal{T}, v \in \mathcal{V}_{k,k+t}, \quad (A32)$$

$$\sum_{i \in \mathcal{N}} u_{k,k+t}^{iv} \leq Q \quad \forall t \in \mathcal{T}, v \in \mathcal{V}_{k,k+t}, \quad (A33)$$

$$u_{k,k+t}^{iv} \leq I^{\max} - \hat{I}_{k,k+t}^i \quad \forall i \in \mathcal{N}, t \in \mathcal{T}, v \in \mathcal{V}_{k,k+t}, \quad (A34)$$

$$\hat{I}_{k,k+t+1}^i = \hat{I}_{k,k+t}^i + \sum_{v \in \mathcal{V}_{k,k+t}} u_{k,k+t}^{iv} - \hat{g}_{k,k+t}^i \quad \forall i \in \mathcal{N}, t \in \mathcal{T}, \quad (A35)$$

$$z_{k,k+t}^{ijv} \in \{0, 1\} \quad \forall t \in \mathcal{T}, v \in \mathcal{V}_{k,k+t}, (i, j) \in E, \quad (A36)$$

$$u_{k,k+t}^{iv} \geq 0 \quad \forall i \in \mathcal{N}, t \in \mathcal{T}, v \in \mathcal{V}_{k,k+t}. \quad (A37)$$

The penalized objective function is Equation (A38) with Constraints (A39) and (A40).

$$\min \sum_{t \in \mathcal{T}} \sum_{(i,j) \in E} \sum_{v \in \mathcal{V}_{k,k+t}} c_{ij} z_{k,k+t}^{ijv} + \sum_{t \in \mathcal{T}} \sum_{i \in \mathcal{N}} (h(\hat{I}_{k,k+t+1}^i)^+ + e(\hat{I}_{k,k+t+1}^i)^-) + \sum_{i \in \mathcal{N}} \sum_{v \in \mathcal{V}} \lambda_k^{iv} (\mu_{k,k}^{iv} + \nu_{k,k}^{iv}), \quad (A38)$$

$$s.t. \mu_{k,k}^{iv} - \nu_{k,k}^{iv} = u_{k,k+t}^{iv} - \bar{u}_{k,k+t}^{iv} \quad \forall i \in \mathcal{N}, v \in \mathcal{V}, \quad (A39)$$

$$\mu_{k,k}^{iv}, \nu_{k,k}^{iv} \geq 0 \quad \forall i \in \mathcal{N}, v \in \mathcal{V}. \quad (A40)$$

Appendix B: Sensitivity Analysis

We show the robustness of ScenPO with regards to varying parameter values for holding and backorder cost parameters. The results are shown in Table A3 on a 5 retailer system. The results show that MQRNN in combination with ScenPO-SS is a robust choice with an average saving of 56.20% among all instances.

Table A3 Results for various holding and backorder cost values.

<i>h</i>	<i>e</i>	Item	PI	EV	EMP	Prediction-Focused Learning			ScenPO-SS			ScenPO-TS		
						MLE	LSTM	MQRNN	MLE	LSTM	MQRNN	MLE	LSTM	MQRNN
0.15	1.5	Transportation cost/Cost	75%	61%	64%	61%	66%	66%	58%	63%	62%	73%	70%	72%
		Holding cost/Cost	25%	25%	29%	26%	25%	23%	38%	28%	31%	18%	14%	15%
		Backorder cost/Cost	0%	14%	7%	13%	9%	11%	4%	9%	6%	9%	16%	13%
		Cost	684	866	890	920	822	831	802	783	775	891	880	863
		ΔCost	0	182	206	236	138	147	118	99	91	207	196	179
		Saving	100%	0%	-13%	-29%	24%	19%	35%	45%	50%	-14%	-8%	2%
		MSE	0	298	726	782	170	181						
		Service	100%	83%	91%	88%	87%	84%	95%	89%	92%	87%	79%	83%
		Time (s)	3	4	4	1	3	3	6	6	5	220	209	173
0.3	1.5	Transportation cost/Cost	79%	59%	59%	57%	64%	63%	55%	61%	61%	66%	67%	67%
		Holding cost/Cost	20%	21%	30%	27%	20%	20%	38%	26%	28%	20%	15%	17%
		Backorder cost/Cost	1%	20%	11%	16%	17%	17%	7%	13%	12%	14%	18%	16%
		Cost	776	1087	1108	1128	1016	1016	1027	958	946	1055	1016	1005
		ΔCost	0	312	332	353	241	240	251	182	170	280	240	229
		Saving	100%	0%	-7%	-13%	23%	23%	19%	41%	45%	10%	23%	26%
		MSE	0	298	726	782	170	181						
		Service	99%	71%	84%	80%	74%	73%	90%	79%	83%	82%	72%	76%
		Time (s)	5	6	6	1	6	6	10	10	9	303	316	233
0.3	3	Transportation cost/Cost	79%	54%	56%	52%	57%	59%	54%	60%	61%	65%	61%	65%
		Holding cost/Cost	21%	19%	27%	25%	18%	19%	41%	27%	29%	23%	14%	17%
		Backorder cost/Cost	0%	27%	17%	22%	25%	23%	5%	12%	10%	12%	25%	18%
		Cost	782	1260	1250	1291	1188	1194	1098	1011	992	1114	1164	1102
		ΔCost	0	478	468	509	406	412	316	229	210	333	382	320
		Saving	100%	0%	2%	-6%	15%	14%	34%	52%	56%	30%	20%	33%
		MSE	0	298	726	782	170	181						
		Service	100%	75%	86%	83%	76%	78%	96%	88%	90%	87%	76%	82%
		Time (s)	5	7	6	1	7	7	10	10	9	1007	1086	808
0.3	6	Transportation cost/Cost	78%	45%	46%	46%	50%	50%	53%	59%	57%	62%	54%	56%
		Holding cost/Cost	20%	15%	22%	23%	17%	15%	43%	31%	34%	21%	13%	14%
		Backorder cost/Cost	2%	40%	32%	32%	33%	35%	4%	11%	9%	17%	32%	30%
		Cost	795	1581	1538	1508	1421	1463	1159	1058	1067	1217	1358	1340
		ΔCost	0	786	744	714	626	668	364	264	273	422	564	546
		Saving	100%	0%	5%	9%	20%	15%	54%	66%	65%	46%	28%	31%
		MSE	0	298	726	782	170	181						
		Service	100%	76%	85%	86%	80%	78%	98%	93%	95%	90%	78%	83%
		Time (s)	5	7	6	1	6	7	9	9	8	384	396	282
0.6	6	Transportation cost/Cost	84%	39%	40%	36%	43%	45%	50%	53%	59%	55%	48%	52%
		Holding cost/Cost	15%	11%	19%	16%	12%	12%	46%	27%	29%	24%	11%	12%
		Backorder cost/Cost	1%	50%	42%	48%	45%	43%	4%	19%	12%	21%	41%	36%
		Cost	870	2093	2064	2265	1825	1815	1496	1372	1302	1516	1722	1630
		ΔCost	0	1223	1193	1395	955	945	626	501	432	646	852	759
		Saving	100%	0%	2%	-14%	22%	23%	49%	59%	65%	47%	30%	38%
		MSE	0	298	726	782	170	181						
		Service	100%	62%	75%	69%	65%	65%	97%	85%	90%	85%	68%	73%
		Time (s)	8	8	9	2	7	7	12	10	12	575	467	361

Appendix C: Complete Experimental Results

Table A4 Detailed numerical results of ScenPO and the proposed benchmarks for a 5-retailer system.

		PI	EV	EMP	Prediction-Focused Learning			ScenPO-SS			ScenPO-TS			
					MLE	LSTM	MQRNN	MLE	LSTM	MQRNN	MLE	LSTM	MQRNN	
5	Random	Cost	718	1183	1207	1284	1166	1152	1013	998	992	1149	1169	1150
		Δ Cost	0	465	489	566	448	434	295	280	274	431	451	432
		Saving	100%	0%	-5%	-22%	4%	6%	36%	40%	41%	7%	3%	7%
		MSE	0	289	638	628	302	299						
		Service	100%	79%	84%	77%	79%	80%	90%	89%	89%	80%	77%	79%
	Time (s)	5	6	5	1	6	6	9	8	8	1109	1095	768	
	Trend	Cost	691	1047	1042	1099	886	873	938	915	774	966	987	906
		Δ Cost	0	356	351	408	195	182	247	224	83	275	296	215
		Saving	100%	0%	2%	-14%	45%	49%	31%	37%	77%	23%	17%	40%
		MSE	0	171	394	476	20	19						
		Service	100%	82%	86%	84%	67%	68%	95%	65%	83%	86%	65%	65%
	Time (s)	3	4	5	1	5	5	8	7	6	1155	658	579	
	Both	Cost	782	1260	1250	1291	1188	1194	1098	1011	992	1114	1164	1102
		Δ Cost	0	478	468	509	406	412	316	229	210	333	382	320
		Saving	100%	0%	2%	-6%	15%	14%	34%	52%	56%	30%	20%	33%
MSE		0	298	726	782	170	181							
Service		100%	75%	86%	83%	76%	78%	96%	88%	90%	87%	76%	82%	
Time (s)	5	7	6	1	7	7	10	10	9	1007	1086	808		
7	Random	Cost	708	1180	1228	1247	1166	1188	987	1017	992	1116	1140	1165
		Δ Cost	0	472	520	539	458	481	279	309	284	408	432	457
		Saving	100%	0%	-10%	-14%	3%	-2%	41%	35%	40%	14%	9%	3%
		MSE	0	289	628	616	302	300						
		Service	100%	79%	81%	81%	79%	78%	94%	89%	89%	82%	78%	80%
	Time (s)	9	12	10	2	12	12	33	26	24	1209	1225	926	
	Trend	Cost	674	1024	1104	1136	881	878	946	912	755	987	989	866
		Δ Cost	0	350	429	461	206	203	272	237	81	312	315	192
		Saving	100%	0%	-23%	-32%	41%	42%	22%	32%	77%	11%	10%	45%
		MSE	0	173	382	505	19	19						
		Service	100%	83%	84%	83%	67%	67%	91%	63%	84%	83%	59%	67%
	Time (s)	8	9	10	2	8	8	30	19	14	1183	754	577	
	Both	Cost	769	1261	1281	1305	1177	1184	1088	1018	986	1144	1106	1123
		Δ Cost	0	493	512	536	408	415	320	249	218	375	338	355
		Saving	100%	0%	-4%	-9%	17%	16%	35%	49%	56%	24%	31%	28%
MSE		0	297	700	765	169	183							
Service		100%	74%	84%	82%	77%	77%	96%	90%	91%	87%	79%	80%	
Time (s)	10	13	10	2	12	12	45	36	26	1187	1138	909		
10	Random	Cost	703	1147	1221	1258	1164	1146	1025	1009	1018	1139	1122	1128
		Δ Cost	0	444	517	555	461	443	321	306	315	435	419	425
		Saving	100%	0%	-17%	-25%	-4%	0%	28%	31%	29%	2%	6%	4%
		MSE	0	290	614	631	302	297						
		Service	100%	79%	81%	81%	77%	80%	90%	88%	88%	79%	79%	79%
	Time (s)	19	40	21	4	42	40	443	376	94	2177	2380	2560	
	Trend	Cost	670	1046	1078	1157	875	875	933	900	776	976	966	902
		Δ Cost	0	376	408	487	206	206	263	230	107	307	296	232
		Saving	100%	0%	-9%	-29%	45%	45%	30%	39%	72%	18%	21%	38%
		MSE	0	173	394	465	19	19						
		Service	100%	82%	85%	81%	66%	66%	93%	66%	80%	84%	63%	65%
	Time (s)	18	18	25	4	20	19	447	139	91	2142	1031	938	
	Both	Cost	766	1280	1265	1308	1186	1181	1082	1029	997	1138	1154	1090
		Δ Cost	0	513	499	542	420	415	315	262	230	371	387	323
		Saving	100%	0%	3%	-5%	18%	19%	39%	49%	55%	28%	25%	37%
MSE		0	294	721	764	167	183							
Service		100%	73%	85%	83%	75%	77%	96%	88%	91%	87%	77%	81%	
Time (s)	28	49	42	8	32	34	564	472	273	3249	2521	2773		

Table A5 Detailed numerical results of ScenPO and the proposed benchmarks for a 7-retailer system.

		PI	EV	EMP	Prediction-Focused Learning			ScenPO-SS			ScenPO-TS			
					MLE	LSTM	MQRNN	MLE	LSTM	MQRNN	MLE	LSTM	MQRNN	
5	<i>Random</i>	Cost	977	1634	1746	1749	1639	1654	1362	1400	1368	1576	1597	1570
		ΔCost	0	657	769	772	662	677	385	424	391	599	620	593
		Saving	100%	0%	-17%	-18%	-1%	-3%	41%	36%	40%	9%	6%	10%
		MSE	0	292	612	627	309	306						
		Service	100%	77%	79%	77%	78%	76%	91%	89%	89%	78%	76%	78%
		Time (s)	14	16	14	3	15	15	35	31	30	1479	1466	1298
	<i>Trend</i>	Cost	902	1418	1417	1470	1174	1165	1231	1208	1022	1311	1332	1150
		ΔCost	0	516	515	568	272	263	329	306	121	409	430	248
		Saving	100%	0%	0%	-10%	47%	49%	36%	41%	77%	21%	17%	52%
		MSE	0	163	386	486	20	19						
		Service	100%	80%	86%	86%	66%	66%	94%	64%	83%	86%	64%	68%
		Time (s)	12	12	12	3	11	11	29	17	16	1412	987	798
	<i>Both</i>	Cost	1061	1750	1774	1833	1633	1621	1500	1412	1385	1552	1581	1550
		ΔCost	0	690	713	773	572	560	439	352	325	491	520	489
		Saving	100%	0%	-3%	-12%	17%	19%	36%	49%	53%	29%	25%	29%
		MSE	0	315	729	809	180	192						
		Service	100%	74%	82%	80%	75%	76%	95%	87%	88%	87%	76%	79%
		Time (s)	19	19	20	4	22	17	84	51	46	1773	1462	1360
7	<i>Random</i>	Cost	964	1609	1713	1803	1610	1655	1373	1379	1368	1560	1582	1599
		ΔCost	0	646	749	840	647	692	410	416	404	597	619	635
		Saving	100%	0%	-16%	-30%	0%	-7%	37%	36%	37%	8%	4%	2%
		MSE	0	293	615	637	310	308						
		Service	100%	78%	80%	75%	77%	75%	90%	88%	89%	78%	75%	78%
		Time (s)	52	105	56	7	92	95	456	414	515	3496	3181	3335
	<i>Trend</i>	Cost	892	1408	1463	1456	1176	1179	1238	1199	1012	1280	1320	1160
		ΔCost	0	516	571	564	284	286	346	307	119	388	428	267
		Saving	100%	0%	-11%	-9%	45%	44%	33%	40%	77%	25%	17%	48%
		MSE	0	166	363	463	20	20						
		Service	100%	80%	85%	86%	66%	65%	95%	64%	83%	86%	64%	67%
		Time (s)	27	26	47	6	25	25	373	120	79	3120	1411	1204
	<i>Both</i>	Cost	1051	1758	1792	1816	1603	1648	1510	1401	1373	1554	1566	1543
		ΔCost	0	707	741	765	552	597	459	350	322	503	515	492
		Saving	100%	0%	-5%	-8%	22%	16%	35%	51%	54%	29%	27%	30%
		MSE	0	316	733	772	179	195						
		Service	100%	75%	82%	80%	76%	74%	96%	87%	89%	86%	76%	79%
		Time (s)	102	196	172	29	104	126	973	702	688	3958	3238	2888
10	<i>Random</i>	Cost	956	1630	1715	1738	1640	1660	1386	1356	1389	1540	1537	1552
		ΔCost	0	674	759	782	683	704	430	400	432	583	581	596
		Saving	100%	0%	-13%	-16%	-1%	-4%	36%	41%	36%	13%	14%	12%
		MSE	0	294	609	637	311	305						
		Service	100%	74%	79%	78%	76%	74%	90%	89%	89%	79%	78%	79%
		Time (s)	354	459	384	65	485	463	1522	1512	1391	4344	4228	3845
	<i>Trend</i>	Cost	883	1410	1442	1485	1172	1169	1240	1192	1032	1318	1276	1151
		ΔCost	0	527	559	602	288	286	357	309	148	435	393	268
		Saving	100%	0%	-6%	-14%	45%	46%	32%	41%	72%	17%	25%	49%
		MSE	0	165	363	474	20	20						
		Service	100%	79%	84%	84%	67%	68%	95%	67%	79%	86%	68%	69%
		Time (s)	269	233	322	55	200	191	1513	1088	1039	4027	2373	2196
	<i>Both</i>	Cost	1041	1835	1865	1806	1620	1637	1485	1404	1366	1573	1545	1516
		ΔCost	0	795	824	765	579	596	444	363	325	532	504	475
		Saving	100%	0%	-4%	4%	27%	25%	44%	54%	59%	33%	37%	40%
		MSE	0	314	722	768	177	195						
		Service	100%	70%	79%	83%	75%	74%	94%	87%	89%	87%	76%	80%
		Time (s)	604	645	649	126	617	609	1567	1555	1484	4426	4241	3798

Table A6 Detailed numerical results of ScenPO and the proposed benchmarks for a 10-retailer system.

		PI	EV	EMP	Prediction-Focused Learning			ScenPO-SS			ScenPO-TS			
					MLE	LSTM	MQRNN	MLE	LSTM	MQRNN	MLE	LSTM	MQRNN	
5	<i>Random</i>	Cost	1290	2302	2454	2662	2325	2358	1844	1877	1849	2152	2226	2143
		Δ Cost	0	1012	1164	1372	1035	1068	553	587	559	862	936	853
		Saving	100%	0%	-15%	-36%	-2%	-6%	45%	42%	45%	15%	8%	16%
		MSE	0	277	570	613	294	290						
		Service	100%	70%	75%	69%	70%	68%	91%	89%	88%	73%	72%	76%
		Time (s)	103	110	88	16	97	115	690	542	615	4587	3977	3833
5	<i>Trend</i>	Cost	1182	2001	2036	2113	1597	1566	1667	1608	1341	1741	1784	1525
		Δ Cost	0	819	854	931	414	383	485	426	159	559	602	343
		Saving	100%	0%	-4%	-14%	49%	53%	41%	48%	81%	32%	26%	58%
		MSE	0	167	363	467	20	19						
		Service	100%	76%	82%	80%	66%	67%	96%	63%	84%	84%	65%	69%
		Time (s)	60	39	62	14	56	58	475	150	115	3242	2224	2177
5	<i>Both</i>	Cost	1400	2567	2597	2746	2305	2342	1999	1887	1872	2247	2297	2201
		Δ Cost	0	1166	1197	1345	904	942	599	487	472	846	897	800
		Saving	100%	0%	-3%	-15%	22%	19%	49%	58%	60%	27%	23%	31%
		MSE	0	322	724	802	183	194						
		Service	100%	68%	77%	72%	69%	69%	96%	87%	88%	82%	69%	74%
		Time (s)	306	243	457	74	302	309	1329	945	976	5184	4356	3800
7	<i>Random</i>	Cost	1287	2321	2481	2656	2378	2381	1839	1871	1851	2171	2296	2175
		Δ Cost	0	1034	1194	1369	1091	1094	552	584	564	884	1009	888
		Saving	100%	0%	-15%	-32%	-5%	-6%	47%	44%	45%	15%	2%	14%
		MSE	0	277	583	613	293	289						
		Service	100%	70%	73%	69%	68%	68%	92%	88%	89%	74%	70%	74%
		Time (s)	562	632	599	103	697	676	1569	1578	1570	5571	5306	3976
7	<i>Trend</i>	Cost	1173	1995	2089	2078	1592	1569	1671	1611	1335	1792	1739	1522
		Δ Cost	0	822	916	905	419	396	498	438	162	619	566	349
		Saving	100%	0%	-11%	-10%	49%	52%	39%	47%	80%	25%	31%	58%
		MSE	0	169	372	469	20	20						
		Service	100%	76%	81%	80%	66%	67%	95%	63%	84%	83%	65%	70%
		Time (s)	357	364	475	83	393	373	1537	1202	1090	4963	3667	2966
7	<i>Both</i>	Cost	1396	2549	2649	2745	2324	2332	2045	1912	1868	2214	2258	2177
		Δ Cost	0	1153	1253	1349	928	936	649	515	472	818	862	780
		Saving	100%	0%	-9%	-17%	19%	19%	44%	55%	59%	29%	25%	32%
		MSE	0	322	745	793	181	196						
		Service	100%	68%	75%	73%	69%	68%	94%	86%	87%	83%	69%	73%
		Time (s)	780	765	808	161	767	785	1621	1594	1610	4772	4951	4000
10	<i>Random</i>	Cost	1287	2339	2502	2646	2360	2356	1871	1852	1853	2223	2289	2254
		Δ Cost	0	1053	1216	1360	1073	1069	585	566	567	937	1003	967
		Saving	100%	0%	-15%	-29%	-2%	-2%	44%	46%	46%	11%	5%	8%
		MSE	0	275	570	622	290	284						
		Service	100%	70%	72%	70%	68%	68%	90%	89%	88%	74%	68%	72%
		Time (s)	805	813	810	161	825	814	1961	1965	1741	6482	6382	5666
10	<i>Trend</i>	Cost	1174	2087	2071	2126	1579	1579	1673	1628	1339	1765	1705	1513
		Δ Cost	0	914	897	952	405	405	499	454	166	591	531	339
		Saving	100%	0%	2%	-4%	56%	56%	45%	50%	82%	35%	42%	63%
		MSE	0	168	377	466	19	20						
		Service	100%	70%	77%	78%	66%	65%	95%	62%	84%	84%	65%	70%
		Time (s)	741	762	784	158	762	756	1925	1945	1689	6085	4214	3822
10	<i>Both</i>	Cost	1396	2606	2689	2778	2298	2350	2036	1918	1873	2240	2245	2164
		Δ Cost	0	1210	1293	1382	902	954	640	522	477	844	849	768
		Saving	100%	0%	-7%	-14%	25%	21%	47%	57%	61%	30%	30%	37%
		MSE	0	319	738	815	177	194						
		Service	100%	67%	74%	73%	70%	67%	94%	87%	88%	83%	70%	74%
		Time (s)	834	926	863	170	856	858	2072	2059	1879	6104	5901	5295

Table A7 Comparison of the various scenario generation approaches for a 5-retailer system.

		PI	EV	residuals-based					quantile-based		
				OLS-ER	OLS-J	OLS-JP	ES	NN	QuantReg	ScenPO	
5	<i>Random</i>	Cost	718	1183	998	989	989	1093	1026	1005	992
		ΔCost	0	465	280	271	271	375	308	287	274
		Saving	100%	0%	40%	42%	42%	19%	34%	38%	41%
		Service	100%	79%	93%	93%	93%	91%	90%	89%	89%
		Time (s)	5	6	8	8	9	7	8	8	8
5	<i>Trend</i>	Cost	691	1047	778	769	768	762	849	775	774
		ΔCost	0	356	87	78	77	71	158	84	83
		Saving	100%	0%	76%	78%	78%	80%	56%	77%	77%
		Service	100%	82%	83%	83%	84%	87%	73%	83%	83%
		Time (s)	3	4	6	6	6	7	6	5	6
5	<i>Both</i>	Cost	782	1260	1023	1020	1014	1100	1006	1007	992
		ΔCost	0	478	241	238	232	318	224	225	210
		Saving	100%	0%	50%	50%	52%	33%	53%	53%	56%
		Service	100%	75%	89%	91%	92%	90%	91%	90%	90%
		Time (s)	5	7	10	10	10	10	10	9	9
7	<i>Random</i>	Cost	708	1180	1012	991	1003	1103	1014	1009	992
		ΔCost	0	472	304	283	295	395	306	301	284
		Saving	100%	-	36%	40%	38%	16%	35%	36%	40%
		Service	100%	79%	91%	94%	92%	91%	90%	89%	89%
		Time (s)	9	12	27	31	39	18	30	23	24
7	<i>Trend</i>	Cost	674	1024	760	758	756	754	843	758	755
		ΔCost	0	350	85	83	82	79	169	84	81
		Saving	100%	0%	76%	76%	77%	77%	52%	76%	77%
		Service	100%	83%	84%	83%	83%	87%	71%	84%	84%
		Time (s)	8	9	17	18	17	18	16	14	14
7	<i>Both</i>	Cost	769	1261	1024	1013	1011	1074	1000	1005	986
		ΔCost	0	493	256	244	242	305	232	236	218
		Saving	100%	0%	48%	50%	51%	38%	53%	52%	56%
		Service	100%	74%	90%	91%	90%	91%	91%	89%	91%
		Time (s)	10	13	39	40	40	32	33	27	26
10	<i>Random</i>	Cost	703	1147	1005	1018	992	1091	1008	1014	1018
		ΔCost	0	444	302	315	289	388	304	310	315
		Saving	100%	-	32%	29%	35%	13%	31%	30%	29%
		Service	100%	79%	91%	92%	94%	92%	90%	89%	88%
		Time (s)	19	40	381	395	441	71	424	91	94
10	<i>Trend</i>	Cost	670	1046	753	763	766	755	844	762	776
		ΔCost	0	376	84	94	96	85	174	93	107
		Saving	100%	0%	78%	75%	75%	77%	54%	75%	72%
		Service	100%	82%	84%	81%	81%	85%	71%	82%	80%
		Time (s)	18	18	139	148	172	166	135	86	91
10	<i>Both</i>	Cost	766	1280	1002	1017	1010	1067	994	1005	997
		ΔCost	0	513	236	250	244	301	227	238	230
		Saving	100%	0%	54%	51%	53%	41%	56%	54%	55%
		Service	100%	73%	92%	91%	91%	92%	92%	89%	91%
		Time (s)	28	49	552	595	567	189	455	374	273

Table A8 Comparison of the various scenario generation approaches for a 7-retailer system.

		PI	EV	residuals-based					quantile-based		
				OLS-ER	OLS-J	OLS-JP	ES	NN	QuantReg	ScenPO	
5	<i>Random</i>	Cost	977	1634	1384	1380	1382	1509	1381	1373	1368
		Δ Cost	0	657	407	403	405	532	404	396	391
		Saving	100%	0%	38%	39%	38%	19%	38%	40%	40%
		Service	100%	77%	91%	92%	92%	91%	90%	89%	89%
		Time (s)	14	16	36	39	51	33	38	31	30
5	<i>Trend</i>	Cost	902	1418	1009	1012	1010	987	1111	1024	1022
		Δ Cost	0	516	107	110	108	85	209	122	121
		Saving	100%	0%	79%	79%	79%	83%	59%	76%	77%
		Service	100%	80%	84%	84%	84%	89%	73%	83%	83%
		Time (s)	12	12	17	17	16	16	16	16	16
5	<i>Both</i>	Cost	1061	1750	1377	1386	1381	1509	1382	1410	1385
		Δ Cost	0	690	316	325	320	448	321	349	325
		Saving	100%	0%	54%	53%	54%	35%	53%	49%	53%
		Service	100%	74%	90%	91%	91%	89%	91%	88%	88%
		Time (s)	19	19	53	62	64	67	53	39	46
7	<i>Random</i>	Cost	964	1609	1376	1403	1384	1511	1385	1390	1368
		Δ Cost	0	646	413	439	420	547	421	426	404
		Saving	100%	0%	36%	32%	35%	15%	35%	34%	37%
		Service	100%	78%	93%	91%	93%	92%	89%	89%	89%
		Time (s)	52	105	547	463	477	328	483	467	515
7	<i>Trend</i>	Cost	892	1408	1007	1011	1013	991	1121	1019	1012
		Δ Cost	0	516	115	119	121	99	229	127	119
		Saving	100%	0%	78%	77%	77%	81%	56%	75%	77%
		Service	100%	80%	83%	82%	82%	87%	73%	81%	83%
		Time (s)	27	26	129	117	130	113	117	75	79
7	<i>Both</i>	Cost	1051	1758	1375	1373	1385	1500	1398	1417	1373
		Δ Cost	0	707	324	322	334	449	347	366	322
		Saving	100%	0%	54%	54%	53%	36%	51%	48%	54%
		Service	100%	75%	91%	92%	91%	90%	89%	86%	89%
		Time (s)	102	196	788	876	853	729	828	636	688
10	<i>Random</i>	Cost	956	1630	1410	1404	1381	1536	1392	1383	1389
		Δ Cost	0	674	454	448	425	579	436	427	432
		Saving	100%	0%	33%	34%	37%	14%	35%	37%	36%
		Service	100%	74%	91%	92%	91%	92%	89%	90%	89%
		Time (s)	354	459	1469	1475	1476	951	1491	1365	1391
10	<i>Trend</i>	Cost	883	1410	998	1014	1020	984	1126	1008	1032
		Δ Cost	0	527	115	131	137	101	243	125	148
		Saving	100%	0%	78%	75%	74%	81%	54%	76%	72%
		Service	100%	79%	84%	81%	80%	88%	70%	82%	79%
		Time (s)	269	233	1155	1088	1105	1117	1092	951	1039
10	<i>Both</i>	Cost	1041	1835	1400	1373	1390	1366	1379	1383	1366
		Δ Cost	0	795	359	332	349	325	338	342	325
		Saving	100%	0%	55%	58%	56%	59%	57%	57%	59%
		Service	100%	70%	89%	91%	89%	89%	90%	87%	89%
		Time (s)	604	645	1550	1523	1559	1484	1550	1495	1484

Table A9 Comparison of the various scenario generation approaches for a 10-retailer system.

		PI	EV	residuals-based					quantile-based		
				OLS-ER	OLS-J	OLS-JP	ES	NN	QuantReg	ScenPO	
5	<i>Random</i>	Cost	1290	2302	1858	1857	1850	2064	1879	1850	1849
		ΔCost	0	1012	568	566	559	773	588	560	559
		Saving	100%	0%	44%	44%	45%	24%	42%	45%	45%
		Service	100%	70%	91%	93%	94%	92%	89%	88%	88%
		Time (s)	103	110	752	690	671	745	606	659	615
5	<i>Trend</i>	Cost	1182	2001	1335	1344	1339	1317	1462	1340	1341
		ΔCost	0	819	152	161	156	134	280	158	159
		Saving	100%	0%	81%	80%	81%	84%	66%	81%	81%
		Service	100%	76%	87%	84%	85%	89%	75%	84%	84%
		Time (s)	60	39	147	151	151	162	163	135	115
5	<i>Both</i>	Cost	1400	2567	1867	1876	1865	2086	1860	1908	1872
		ΔCost	0	1166	467	475	465	685	459	507	472
		Saving	100%	0%	60%	59%	60%	41%	61%	57%	60%
		Service	100%	68%	90%	91%	90%	89%	89%	87%	88%
		Time (s)	306	243	1062	1059	1093	1048	1006	954	976
7	<i>Random</i>	Cost	1287	2321	1914	1861	1891	2054	1899	1854	1851
		ΔCost	0	1034	627	574	604	767	612	567	564
		Saving	100%	0%	39%	44%	42%	26%	41%	45%	45%
		Service	100%	70%	91%	93%	92%	91%	89%	89%	89%
		Time (s)	562	632	1551	1546	1549	1399	1574	1576	1570
7	<i>Trend</i>	Cost	1173	1995	1331	1321	1325	1314	1489	1351	1335
		ΔCost	0	822	158	147	152	141	316	178	162
		Saving	100%	0%	81%	82%	82%	83%	62%	78%	80%
		Service	100%	76%	85%	85%	85%	89%	74%	82%	84%
		Time (s)	357	364	1265	1167	1203	1195	1202	1032	1090
7	<i>Both</i>	Cost	1396	2549	1877	1881	1873	2068	1875	1912	1868
		ΔCost	0	1153	481	484	477	672	479	516	472
		Saving	100%	0%	58%	58%	59%	42%	58%	55%	59%
		Service	100%	68%	91%	91%	91%	89%	89%	86%	87%
		Time (s)	780	765	1632	1638	1621	1629	1635	1616	1610
10	<i>Random</i>	Cost	1287	2339	1889	1893	1867	2041	1852	1872	1853
		ΔCost	0	1053	603	606	580	754	566	586	567
		Saving	100%	0%	43%	42%	45%	28%	46%	44%	46%
		Service	100%	70%	91%	91%	92%	93%	90%	89%	88%
		Time (s)	805	813	1900	1920	1931	1673	1906	1784	1741
10	<i>Trend</i>	Cost	1174	2087	1346	1342	1340	1321	1504	1336	1339
		ΔCost	0	914	172	168	166	148	330	162	166
		Saving	100%	0%	81%	82%	82%	84%	64%	82%	82%
		Service	100%	70%	85%	83%	85%	88%	72%	83%	84%
		Time (s)	741	762	1860	1901	1902	1891	1821	1691	1689
10	<i>Both</i>	Cost	1396	2606	1908	1901	1916	2055	1875	1917	1873
		ΔCost	0	1210	512	505	520	659	479	521	477
		Saving	100%	0%	58%	58%	57%	46%	60%	57%	61%
		Service	100%	67%	89%	89%	89%	90%	88%	86%	88%
		Time (s)	834	926	2084	2051	2067	1845	2097	1893	1879

Table A10 Detailed numerical results of CombOptNet for a 5-retailer system.

		PI	EV	EMP	Prediction-Focused Learning			ScenPO-SS			ScenPO-TS			CombOptNet
					MLE	LSTM	MQRNN	MLE	LSTM	MQRNN	MLE	LSTM	MQRNN	
<i>Random</i>	Cost	718	1183	1207	1284	1166	1152	1013	998	992	1149	1169	1150	1234
	Δ Cost	0	465	489	566	448	434	295	280	274	431	451	432	516
	Saving	100%	0%	-5%	-22%	4%	6%	36%	40%	41%	7%	3%	7%	-11%
	Service	100%	79%	84%	77%	79%	80%	90%	89%	89%	80%	77%	79%	96%
	Time (s)	5	6	5	1	6	6	9	8	8	1109	1095	768	5
<i>Trend</i>	Cost	691	1047	1042	1099	886	873	938	915	774	966	987	906	1051
	Δ Cost	0	356	351	408	195	182	247	224	83	275	296	215	360
	Saving	100%	0%	2%	-14%	45%	49%	31%	37%	77%	23%	17%	40%	-1%
	Service	100%	82%	86%	84%	67%	68%	95%	65%	83%	86%	65%	65%	81%
	Time (s)	3	4	5	1	5	5	8	7	6	1155	658	579	6
<i>Both</i>	Cost	782	1260	1250	1291	1188	1194	1098	1011	992	1114	1164	1102	1193
	Δ Cost	0	478	468	509	406	412	316	229	210	333	382	320	411
	Saving	100%	0%	2%	-6%	15%	14%	34%	52%	56%	30%	20%	33%	14%
	Service	100%	75%	86%	83%	76%	78%	96%	88%	90%	87%	76%	82%	84%
	Time (s)	5	7	6	1	7	7	10	10	9	1007	1086	808	6
Inst-1	Cost	413	2198	2390	2513	1519	1788	3011	4445	1464	2278	3407	2241	2227
	Δ Cost	0	1784	1977	2100	1106	1375	2598	4032	1051	1865	2993	1827	2227
	Saving	100%	0%	-11%	-18%	38%	23%	-46%	-126%	41%	-5%	-68%	-2%	-25%
	Service	97%	77%	74%	92%	85%	75%	99%	100%	95%	91%	94%	74%	77%
	Time (s)	2	0	0	0	1	1	2	1	3	792	778	653	3
Inst-2	Cost	3980	8554	9320	10345	7257	8209	7514	7955	6436	9897	11410	9521	10361
	Δ Cost	0	4574	5340	6365	3277	4229	3534	3976	2456	5917	7430	5542	10361
	Saving	100%	0%	-17%	-39%	28%	8%	23%	13%	46%	-29%	-62%	-21%	-127%
	Service	98%	71%	71%	69%	79%	67%	85%	96%	88%	67%	65%	60%	62%
	Time (s)	7	4	1	0	6	6	5	2	5	1262	927	1066	6

Table A11 Detailed numerical results of ScenPO and the proposed benchmarks for real-life Instance 1.

#Retailer	ℓ	Item	PI	EV	EMP	Prediction-Focused Learning			ScenPO-SS			ScenPO-TS		
						MLE	LSTM	MQRNN	MLE	LSTM	MQRNN	MLE	LSTM	MQRNN
5	5	Cost	413	2198	2390	2513	1519	1788	3011	4445	1464	2278	3407	2241
		Δ Cost	0	1784	1977	2100	1106	1375	2598	4032	1051	1865	2993	1827
		Saving	100%	0%	-11%	-18%	38%	23%	-46%	-126%	41%	-5%	-68%	-2%
		MSE	0	58	112	282	33	39						
		Service	97%	77%	74%	92%	85%	75%	99%	100%	95%	91%	94%	74%
		Time (s)	2	0	0	0	1	1	2	1	3	792	778	653
	7	Cost	349	2097	2365	2634	1550	1803	3075	4634	1377	2164	3515	1869
		Δ Cost	0	1748	2016	2285	1200	1454	2725	4284	1028	1815	3166	1520
		Saving	100%	0%	-15%	-31%	31%	17%	-56%	-145%	41%	-4%	-81%	13%
		MSE	0	54	116	315	29	35						
		Service	100%	77%	70%	94%	83%	72%	99%	100%	96%	91%	91%	75%
		Time (s)	4	1	0	0	4	1	3	1	4	940	864	723
	10	Cost	351	2116	2504	2866	1542	1807	3102	4673	1285	2385	3140	1881
		Δ Cost	0	1764	2153	2515	1191	1456	2751	4322	933	2034	2789	1529
		Saving	100%	0%	-22%	-43%	33%	17%	-56%	-145%	47%	-15%	-58%	13%
		MSE	0	49	113	320	25	28						
		Service	100%	77%	69%	90%	85%	76%	99%	100%	95%	93%	88%	75%
		Time (s)	6	2	1	0	6	4	3	1	4	1050	961	712
7	5	Cost	481	4363	4604	5708	2735	3384	4831	5936	2014	5470	6737	4226
		Δ Cost	0	3882	4123	5227	2254	2903	4350	5455	1533	4989	6256	3745
		Saving	100%	0%	-6%	-35%	42%	25%	-12%	-41%	61%	-29%	-61%	4%
		MSE	0	98	176	332	37	40						
		Service	98%	72%	74%	86%	80%	70%	95%	100%	95%	83%	84%	66%
		Time (s)	10	6	2	1	16	9	8	4	13	1376	1093	1201
	7	Cost	416	4250	5375	5926	2812	3411	5163	6008	1892	5234	7081	3716
		Δ Cost	0	3834	4959	5510	2396	2996	4747	5592	1476	4818	6666	3300
		Saving	100%	0%	-29%	-44%	38%	22%	-24%	-46%	62%	-26%	-74%	14%
		MSE	0	98	185	324	33	37						
		Service	100%	72%	66%	87%	80%	69%	92%	100%	96%	86%	83%	69%
		Time (s)	15	8	4	2	23	11	11	4	13	1494	1195	1217
	10	Cost	417	4295	4580	5802	2794	3398	4654	6119	1747	5584	6886	3604
		Δ Cost	0	3877	4163	5385	2377	2981	4237	5701	1330	5167	6468	3187
		Saving	100%	0%	-7%	-39%	39%	23%	-9%	-47%	66%	-33%	-67%	18%
		MSE	0	98	177	322	30	35						
		Service	100%	72%	65%	84%	80%	72%	95%	99%	94%	84%	87%	68%
		Time (s)	21	12	5	4	35	14	15	5	14	1565	1889	1234
10	5	Cost	570	7785	8937	9537	5006	6243	6888	7979	3516	9516	11195	8627
		Δ Cost	0	7215	8367	8968	4436	5674	6318	7409	2947	8946	10625	8057
		Saving	100%	0%	-16%	-24%	39%	21%	12%	-3%	59%	-24%	-47%	-12%
		MSE	0	137	260	368	59	64						
		Service	99%	69%	66%	79%	78%	70%	93%	100%	92%	77%	75%	61%
		Time (s)	27	35	18	6	30	28	20	8	25	2133	2823	2165
	7	Cost	501	7693	7864	9401	5038	6154	7274	7946	3182	9020	10427	7479
		Δ Cost	0	7192	7362	8900	4537	5653	6773	7445	2681	8519	9926	6977
		Saving	100%	0%	-2%	-24%	37%	21%	6%	-4%	63%	-18%	-38%	3%
		MSE	0	136	251	364	55	61						
		Service	100%	69%	70%	80%	78%	67%	91%	100%	94%	77%	78%	67%
		Time (s)	41	53	18	8	45	41	29	9	30	3764	3664	2854
	10	Cost	585	7697	8917	9296	5027	6846	7006	7971	3097	9571	10188	7579
		Δ Cost	0	7111	8332	8711	4441	6261	6420	7386	2511	8985	9602	6993
		Saving	100%	0%	-17%	-22%	38%	12%	10%	-4%	65%	-26%	-35%	2%
		MSE	0	137	239	376	50	58						
		Service	98%	69%	68%	82%	78%	69%	91%	100%	93%	78%	82%	63%
		Time (s)	87	88	32	19	109	60	50	13	30	5363	5201	3086

Table A12 Detailed numerical results of ScenPO and the proposed benchmarks for real-life Instance 2.

#Retailer	ℓ	Item	PI	EV	EMP	Prediction-Focused Learning			ScenPO-SS			ScenPO-TS		
						MLE	LSTM	MQRNN	MLE	LSTM	MQRNN	MLE	LSTM	MQRNN
5	5	Cost	3980	8554	9320	10345	7257	8209	7514	7955	6436	9897	11410	9521
		Δ Cost	0	4574	5340	6365	3277	4229	3534	3976	2456	5917	7430	5542
		Saving	100%	0%	-17%	-39%	28%	8%	23%	13%	46%	-29%	-62%	-21%
		MSE	0	300	514	465	179	175						
		Service	98%	71%	71%	69%	79%	67%	85%	96%	88%	67%	65%	60%
		Time (s)	7	4	1	0	6	6	5	2	5	1262	927	1066
	7	Cost	3970	8416	10176	8705	7507	7808	7497	7700	6125	9354	8579	7958
		Δ Cost	0	4447	6206	4735	3537	3838	3528	3730	2155	5384	4609	3988
		Saving	100%	0%	-40%	-6%	20%	14%	21%	16%	52%	-21%	-4%	10%
		MSE	0	285	438	473	158	156						
		Service	99%	72%	69%	69%	79%	71%	85%	97%	85%	65%	71%	65%
		Time (s)	18	9	3	0	13	10	6	3	7	1598	1173	2771
	10	Cost	4013	8559	9976	9563	7445	7807	6940	8297	6415	9399	9900	8413
		Δ Cost	0	4546	5963	5550	3432	3794	2928	4284	2402	5386	5888	4400
		Saving	100%	0%	-31%	-22%	25%	17%	36%	6%	47%	-18%	-30%	3%
		MSE	0	267	427	473	133	130						
		Service	99%	68%	65%	67%	78%	73%	87%	95%	87%	61%	65%	65%
		Time (s)	60	30	4	1	64	17	6	4	7	3193	1152	3465
7	5	Cost	4874	10794	10924	11758	9241	9287	9155	10040	7831	11876	14236	11784
		Δ Cost	0	5920	6051	6884	4367	4414	4281	5166	2957	7003	9363	6911
		Saving	100%	0%	-2%	-16%	26%	25%	28%	13%	50%	-18%	-58%	-17%
		MSE	0	267	421	460	164	169						
		Service	99%	68%	75%	75%	79%	75%	89%	99%	88%	74%	66%	65%
		Time (s)	24	27	5	2	27	14	16	5	11	2391	3628	2421
	7	Cost	4836	10535	11767	11297	9485	9620	9345	10605	7948	11756	12798	11075
		Δ Cost	0	5699	6931	6461	4649	4784	4509	5769	3112	6920	7962	6239
		Saving	100%	0%	-22%	-13%	18%	16%	21%	-1%	45%	-21%	-40%	-9%
		MSE	0	249	386	414	143	147						
		Service	99%	72%	70%	81%	76%	74%	88%	97%	85%	77%	77%	69%
		Time (s)	151	108	10	8	134	40	19	5	19	4743	4867	4756
	10	Cost	4826	10797	11954	11604	9126	9693	9398	10402	8005	11614	13831	10451
		Δ Cost	0	5971	7128	6779	4300	4867	4572	5576	3179	6789	9005	5625
		Saving	100%	0%	-19%	-14%	28%	18%	23%	7%	47%	-14%	-51%	6%
		MSE	0	232	355	422	120	124						
		Service	99%	70%	67%	77%	78%	74%	87%	98%	87%	73%	75%	70%
		Time (s)	440	433	28	44	415	337	34	6	39	6866	5637	6658
10	5	Cost	6417	14953	15874	15825	12435	13543	12508	14101	10183	16047	18480	17328
		Δ Cost	0	8535	9457	9408	6017	7126	6090	7683	3765	9630	12063	10910
		Saving	100%	0%	-11%	-10%	30%	17%	29%	10%	56%	-13%	-41%	-28%
		MSE	0	225	363	420	128	135						
		Service	100%	68%	68%	78%	77%	70%	90%	98%	89%	75%	71%	62%
		Time (s)	434	336	48	34	516	215	244	9	250	7472	7166	8594
	7	Cost	6574	15122	15824	16201	12380	13179	12724	13985	10255	15986	19548	15029
		Δ Cost	0	8548	9249	9627	5806	6605	6150	7411	3681	9412	12974	8455
		Saving	100%	0%	-8%	-13%	32%	23%	28%	13%	57%	-10%	-52%	1%
		MSE	0	212	379	407	113	118						
		Service	97%	67%	70%	80%	77%	70%	89%	100%	87%	74%	74%	66%
		Time (s)	937	866	263	136	1208	832	347	11	511	8431	8788	9257
	10	Cost	6411	15103	15285	16140	12130	13320	12915	13981	10395	15337	18126	15936
		Δ Cost	0	8692	8874	9729	5719	6908	6504	7570	3984	8926	11715	9525
		Saving	100%	0%	-2%	-12%	34%	21%	25%	13%	54%	-3%	-35%	-10%
		MSE	0	201	359	410	97	102						
		Service	99%	68%	74%	74%	77%	72%	89%	99%	89%	79%	79%	66%
		Time (s)	1194	1345	633	233	1348	1265	912	23	774	10487	8931	9936

Table A13 Comparison of the various scenario generation approaches for real-life Instance 1.

#Retailer	ℓ	Item	PI	EV	residuals-based					quantile-based	
					OLS-ER	OLS-J	OLS-JP	ES	NN	QuantReg	ScenPO
5	5	Cost	413	2198	3292	2211	2208	3002	2224	1615	1464
		Δ Cost	0	1784	2879	1798	1795	2589	1810	1201	1051
		Saving	100%	0%	-61%	-1%	-1%	-45%	-1%	33%	41%
		Service	97%	77%	99%	96%	96%	99%	99%	93%	95%
		Time (s)	2	0	2	2	2	2	3	2	3
	7	Cost	349	2097	3034	2432	2434	2872	2305	1472	1377
		Δ Cost	0	1748	2685	2082	2084	2522	1956	1123	1028
		Saving	100%	0%	-54%	-19%	-19%	-44%	-12%	36%	41%
		Service	100%	77%	99%	97%	97%	98%	99%	91%	96%
		Time (s)	4	1	1	3	3	2	4	2	4
	10	Cost	351	2116	2997	2260	2261	2366	2308	1423	1285
		Δ Cost	0	1764	2645	1909	1910	2015	1956	1072	933
Saving		100%	0%	-50%	-8%	-8%	-14%	-11%	39%	47%	
Service		100%	77%	99%	98%	98%	99%	99%	91%	95%	
Time (s)		6	2	2	5	5	4	5	2	4	
7	5	Cost	481	4363	4784	3367	3420	4093	3172	2299	2014
		Δ Cost	0	3882	4303	2886	2939	3612	2691	1818	1533
		Saving	100%	0%	-11%	26%	24%	7%	31%	53%	61%
		Service	98%	72%	96%	93%	93%	99%	95%	93%	95%
		Time (s)	10	6	4	10	10	8	13	5	13
	7	Cost	416	4250	4852	3706	3681	4001	3300	2393	1892
		Δ Cost	0	3834	4437	3290	3265	3585	2884	1978	1476
		Saving	100%	0%	-16%	14%	15%	6%	25%	48%	62%
		Service	100%	72%	95%	93%	94%	97%	96%	89%	96%
		Time (s)	15	8	7	15	14	11	17	6	13
	10	Cost	417	4295	4272	3349	3532	3351	3453	2274	1747
		Δ Cost	0	3877	3854	2931	3114	2934	3035	1857	1330
Saving		100%	0%	1%	24%	20%	24%	22%	52%	66%	
Service		100%	72%	95%	94%	95%	97%	95%	90%	94%	
Time (s)		21	12	12	21	20	18	24	7	14	
10	5	Cost	570	7785	6596	5253	5244	5903	4895	4200	3516
		Δ Cost	0	7215	6026	4684	4674	5333	4326	3630	2947
		Saving	100%	0%	16%	35%	35%	26%	40%	50%	59%
		Service	99%	69%	94%	91%	91%	96%	93%	90%	92%
		Time (s)	27	35	17	26	25	21	31	18	25
	7	Cost	501	7693	7019	5701	5732	5894	4991	4183	3182
		Δ Cost	0	7192	6517	5200	5231	5393	4490	3682	2681
		Saving	100%	0%	9%	28%	27%	25%	38%	49%	63%
		Service	100%	69%	93%	92%	93%	94%	93%	88%	94%
		Time (s)	41	53	26	39	44	29	44	22	30
	10	Cost	585	7697	6551	5455	5551	5240	5091	4251	3097
		Δ Cost	0	7111	5966	4870	4965	4654	4506	3666	2511
Saving		100%	0%	16%	32%	30%	35%	37%	48%	65%	
Service		98%	69%	93%	93%	92%	93%	94%	88%	93%	
Time (s)		87	88	51	70	73	45	106	23	30	

Table A14 Comparison of the various scenario generation approaches for real-life Instance 2.

#Retailer	ℓ	Item	PI	EV	residuals-based					quantile-based	
					OLS-ER	OLS-J	OLS-JP	ES	NN	QuantReg	ScenPO
5	5	Cost	3980	8554	7050	6827	6588	6914	6625	6689	6436
		Δ Cost	0	4574	3070	2847	2608	2934	2646	2709	2456
		Saving	100%	0%	33%	38%	43%	36%	42%	41%	46%
		Service	98%	71%	89%	85%	84%	89%	86%	83%	88%
	Time (s)	7	4	3	5	6	5	6	2	5	
	7	Cost	3970	8416	6742	7027	7346	6991	6392	6643	6125
		Δ Cost	0	4447	2772	3058	3377	3021	2423	2673	2155
		Saving	100%	0%	38%	31%	24%	32%	46%	40%	52%
		Service	99%	72%	93%	87%	85%	89%	89%	85%	85%
	Time (s)	18	9	6	11	11	8	14	5	7	
	10	Cost	4013	8559	6710	6652	6998	7058	6639	6870	6415
		Δ Cost	0	4546	2698	2639	2985	3046	2627	2857	2402
Saving		100%	0%	41%	42%	34%	33%	42%	37%	47%	
Service		99%	68%	88%	87%	85%	87%	87%	82%	87%	
Time (s)	60	30	21	26	23	10	72	6	7		
7	5	Cost	4874	10794	9538	8553	8525	9049	8327	8423	7831
		Δ Cost	0	5920	4664	3679	3651	4175	3453	3550	2957
		Saving	100%	0%	21%	38%	38%	29%	42%	40%	50%
		Service	99%	68%	92%	88%	89%	91%	89%	85%	88%
	Time (s)	24	27	8	15	20	21	17	9	11	
	7	Cost	4836	10535	8870	8711	8688	8977	8409	8697	7948
		Δ Cost	0	5699	4034	3875	3852	4141	3573	3861	3112
		Saving	100%	0%	29%	32%	32%	27%	37%	32%	45%
		Service	99%	72%	92%	88%	87%	93%	89%	85%	85%
	Time (s)	151	108	46	98	83	28	76	16	19	
	10	Cost	4826	10797	8814	8681	8464	9213	8569	8270	8005
		Δ Cost	0	5971	3989	3855	3639	4387	3744	3444	3179
Saving		100%	0%	33%	35%	39%	27%	37%	42%	47%	
Service		99%	70%	92%	88%	91%	88%	90%	83%	87%	
Time (s)	440	433	174	321	260	151	722	24	39		
10	5	Cost	6417	14953	12430	11789	11786	11776	11317	11179	10183
		Δ Cost	0	8535	6012	5371	5369	5359	4900	4762	3765
		Saving	100%	0%	30%	37%	37%	37%	43%	44%	56%
		Service	100%	68%	93%	89%	89%	92%	88%	86%	89%
	Time (s)	434	336	119	351	360	292	650	38	250	
	7	Cost	6574	15122	12022	11472	11663	12032	11249	10961	10255
		Δ Cost	0	8548	5448	4898	5089	5458	4674	4387	3681
		Saving	100%	0%	36%	43%	40%	36%	45%	49%	57%
		Service	97%	67%	92%	89%	90%	93%	92%	86%	87%
	Time (s)	937	866	584	1129	1103	537	1187	206	511	
	10	Cost	6411	15103	11805	11514	11826	11667	11485	11015	10395
		Δ Cost	0	8692	5394	5103	5415	5256	5074	4604	3984
Saving		100%	0%	38%	41%	38%	40%	42%	47%	54%	
Service		99%	68%	92%	88%	89%	90%	91%	85%	89%	
Time (s)	1194	1345	1167	1864	1948	1298	2414	628	774		